IEEE Access
Multidisciplinary : Rapid Review : Open Access Journal

Received 20 July 2023, accepted 9 September 2023, date of publication 15 September 2023, date of current version 16 October 2023.

Digital Object Identifier 10.1109/ACCESS.2023.3315747

RESEARCH ARTICLE

Profit Expansion of a Solar Integrated Day-Ahead System by Placement of TCSC and Fuel Cell in the Presence of Disequilibrium Price

SUBHOJIT DAWN[1], SHREYA SHREE DAS[2], (Graduate Student Member, IEEE), M. RAMESH[3], (Member, IEEE), SAI RAM INKOLLU[4], THANDAVA KRISHNA SAI PANDRAJU[5], FAISAL ALSAIF[6], SAGER ALSULAMY[7], AND TAHA SELIM USTUN[8], (Member, IEEE)

[1]Department of Electrical and Electronics Engineering, Velagapudi Ramakrishna Siddhartha Engineering College, Vijayawada, Andhra Pradesh 520007, India
[2]School of Electronics Engineering, VIT-AP University, Amaravati, Andhra Pradesh 522237, India
[3]Department of Electrical and Electronic Engineering, Marri Laxman Reddy Institute of Technology and Management, Hyderabad, Telangana 500043, India
[4]Department of Electrical and Electronics Engineering, R. K. College of Engineering, Kethanakonda, Andhra Pradesh 521456, India
[5]Department of Electrical and Electronics Engineering, Dhanekula Institute of Engineering and Technology, Gangur, Andhra Pradesh 521139, India
[6]Department of Electrical Engineering, College of Engineering, King Saud University, Riyadh 11421, Saudi Arabia
[7]Energy and Climate Change Division, Sustainable Energy Research Group, Faculty of Engineering and Physical Sciences, University of Southampton, SO17 1BJ Southampton, U.K.
[8]Fukushima Renewable Energy Institute (FREA), National Institute of Advanced Industrial Science and Technology (AIST), Koriyama 100-8921, Japan

Corresponding authors: Subhojit Dawn (subhojit.dawn@gmail.com) and Taha Selim Ustun (selim.ustun@aist.go.jp)

This work was supported by the Researchers Supporting Project through King Saud University, Riyadh, Saudi Arabia, under Grant RSPD2023R646.

ABSTRACT The usage of renewable energy sources in the power sector has increased day by day to preserve non-renewable resources from extinction. The growth of earnings in the electricity market has also become a critical part as the electricity generated from the renewable integrated system is fluctuating in nature. For a renewable-associated system, energy is abundant during low-demand hours. These excess units are available due to the presence of renewable energy sources like solar, wind, etc. So, a better way to manage this situation is to store the excess energy in the storage devices and use that energy in high-demand hours to enhance the system's economic profit. This paper presents a comparative study of system economic parameters between regulated and deregulated renewable-associated systems. Solar power has been considered here as a renewable energy source due to its high efficiency and easy availability nature. This work also focused on maximizing the system profit in a deregulated system by the placement of a Thyristor Controlled Series Compensator (TCSC) along with the fuel cell in the presence of a disequilibrium price (DP). The disequilibrium price has occurred due to the disparity of real and expected renewable data which controls the entire renewable-associated system. To achieve maximum profit, it is imperative to reduce generation expenses to a minimum. A flexible alternating current transmission system (FACTS) is used to enhance and increase the system's power transfer capability and controllability. The system voltage profile and the scenarios of location-based marginal price (LBMP) with and without consideration of TCSC have also been deployed in this work. The study has been performed with different optimization techniques such as Sequential Quadratic Programming (SQP) and Artificial Bee Colony Algorithms (ABC) to analyze the economic risk of the system with a modified IEEE 14-bus system.

INDEX TERMS Deregulation, solar photovoltaic, fuel cell, disequilibrium price, system profit, revenue, FACTS devices, TCSC.

The associate editor coordinating the review of this manuscript and approving it for publication was Ozan Erdinç.

I. INTRODUCTION

Over recent years, the deregulated power system has replaced the monopoly in the electricity market. The system creates competition among the market participants which give benefit to the customers. The incorporation of renewable energy encourages the power industry's transition from a monopoly to a competitive power system. Renewable sources have a large potential to make an impact by adding energy supply, managing the demand & supply ratio, and preserving the environment. Solar PV is preferred utmost for power generation due to several significant advantages such as its abundance, zero carbon footprint, and reliable nature. Solar PV has an unpredictable nature like other renewable sources which can cause risk in the system associated with power system operation (e.g., frequency and voltage stability, etc.) or liabilities associated with disequilibrium price. Further additional renewable sources and storage devices are integrated into the system to increase stability by providing power supply and counteract the impacts of disequilibrium prices in the system. The limitation on the installation of new transmission lines allows the electric operators to improve their techniques to maximize the flow of power through existing transmission lines. The most adaptable and practical option for controlling the movement of power along transmission lines is FACTS equipment.

Many challenges are been observed in the area of operation of renewable sources, storage devices, and FACTS devices in a deregulated system. Weber et al. [1] deliberate the challenges and achievements faced in deregulating the electricity industry and the negative outcomes that can result from it. It provides a comprehensive literature review of the problems experienced in various deregulation efforts and advises countries to carefully consider these obstacles before implementing deregulation. Reference [2] proposes a strategy for the coordination of wind-based power resources with energy storage systems to optimize their participation in wholesale electricity markets. A bi-level programming framework is proposed to maximize the expected profit of a Virtual Power Plant (VPP) consisting of multiple Wind Producers (WPs) and a Battery Energy Storage System (BESS). Paper [3] includes a two-stage stochastic programming model for day-ahead scheduling and a predictive real-time dispatch model for operational management. The framework is applied to two distribution systems to investigate the DSO's level of risk exposure while minimizing its total cost. Gao and Ai [4] proposed a modeling and optimization method for microgrids that considers the source, load, storage, and full-time collaborative optimization within and outside the microgrid. Reference [5] examines the impact of energy imbalances on financial rewards in peer-to-peer electricity markets. It proposes a new symmetric imbalance charge mechanism that penalizes market participants irrespective of the direction of their energy imbalance, providing a financial incentive for them to reduce their energy imbalances. Reference [6] deliberates on the impact of renewable energy source integration on the system economy in a deregulated power market.

Paper [7] depicts the challenges faced by utilities in managing power quality, voltage stabilization, and efficient energy utilization with the emerging use of renewable and distributed energy sources. An Improved Frequency Regulation (IFR) for an interconnected hybrid power system under a deregulated scenario is proposed in [8]. Reference [9] discusses the process of deregulation in the energy power market, which aims to increase efficiency and competition among stakeholders. It also explains how suppliers' profits are maximized while customers' payments are reduced by adopting a bidding strategy. A hybrid fuzzy-PSO prediction model for solar PV and wind power generation in microgrid systems and distribution networks is deliberated by Teferra et al. [10]. However, reference [11] aims to enhance the transfer capability of existing power networks to satisfy the increased power demand by using the Cuckoo Optimization Algorithm. Reference [12] has anticipated the optimal power flow problem with the optimal integration of wind turbines, photovoltaic systems, and TCSC in power systems. In [13], a multi-objective strategy has been depicted for managing transmission congestion in power systems by optimizing the capabilities of distributed generators (DG) and rescheduling conventional generators. Reference [14] discusses the optimization of hydro and wind power portfolios in real-time market operations. It proposes the use of internal balancing of complementary imbalances. Zhu et al. [15] deliver an overview of the deregulated energy market and the challenges faced by market participants in this domain. It highlights the potential of reinforcement learning techniques to address these challenges and improve the efficiency of energy market operations. A bidding strategy model for a Battery Energy Storage System (BESS) in a Joint Active and Reactive Power Market (JARPM) in the Day-Ahead-Market (DAM) and the Real-Time-Market (RTM) using a robust framework is described in [16] to maximize the BESS owner's profit while facing price uncertainty.

The use of metaheuristic algorithms to solve the optimal power flow problem with the presence of FACTS devices in the power system is discussed by [17]. Zhang et al. [18] explore a bi-level multi-mode power management strategy to improve the efficiency, remaining life, and life-cycle cost of multi-stack fuel cell battery hybrid power systems. Peng et al. [19] propose an approach to a hierarchical energy management strategy for fuel cell-based heavy-duty hybrid power systems to enhance fuel economy and durability. Reference [20] highlights the involvement of the system operator (SO) in the balancing market (BM) for renewable energy generation and suggests that intermittent-renewable generators will have to actively participate in the balancing market and be part of the solution as well as the cause. Paper [21] discusses the decreasing costs of renewable energies, particularly wind power and photovoltaic, and their economic issues from a system perspective. The uncertain and intermittent nature of these technologies requires continuous compensation by other flexible/balancing resources, which may incur significant balancing costs. Akinyele et al. [22] review the potential of fuel cells (FCs) for microgrid systems, which are decentralized energy systems and can help mitigate energy poverty in remote locations. Reference [23] presents a standalone hybrid solar/wind/fuel cell power generation system for remote areas. It combines solar and wind energy with a fuel cell system to produce electric energy.

Shamsi and Cuffe [24] have formulated a trading strategy in a prediction market to compensate for the imbalance costs in the electricity market by combining the payouts of two venues. Considering the exposure of both wind power plants (WPP) and conventional suppliers to imbalance prices and achieving Nash equilibrium to determine the option contract specifications. An optimal combined sharing strategy of fuel cell/wind turbine/battery storage unit and demand response as microgrids to improve all of their profit in market participation is proposed in [25]. Paper [26] presents a model predictive control algorithm that operates a Hydrogen-based Energy Storage System paired with a wind farm to smooth power injection into the grid. Reference [27] studies an integrated energy system that includes hydrogen as an energy vector and hydrogen storage.

The comprehensive literature survey indicates that relatively limited works have been conducted by researchers on the integration of solar PV and energy storage devices in a deregulated system. A few concepts are examined yet in this field which have been explored in a broad way in this work.

This paper discusses the incorporation of renewable energy into the existing electrical system, which is vital in a competitive electrical system. The inclusion of renewable resources assisted the power sector's transformation from a monopoly to a competitive one. The paper aims to investigate system generation costs, profit, voltage profiles, and LBMP in a deregulated power market incorporating solar photovoltaics & fuel cells along with the optimal placement of TCSC. The fuel cell has been used here as a reserve generating unit to mitigate the deficit of power in the renewable incorporated system. A regulated power market is one where the government sets the prices and regulates the supply and demand of electricity. In contrast, a deregulated power market is one where the prices are determined by the market forces of supply and demand, and the government does not regulate the prices. The key objectives of the work are as follows:

- In a solar-associated deregulated power market, generating companies (GENCOs) and distribution companies (DISCOs) enter into a power supply agreement based on solar irradiance and temperature estimation. However, if the real solar radiation and temperature differ from the expected data, there may be a shortfall or extra in power delivery by the GENCOs, which can result in a disequilibrium price (DP). The ISO (Independent System Operator) may penalize or reward the GENCOs for this disequilibrium price.
- Hence, GENCOs are trying to reduce the power difference between real and expected solar power to decrease the negative consequences of disequilibrium price rice.
- The most efficient technique to deal with the present power issue is with an energy storage system. In a global power market, storage systems can reduce power inconsistencies and the strain on thermal power plants, allowing economic benefit to be achieved. In this scenario, a fuel cell is used to mitigate the detrimental impacts of cost inequalities in the hybrid thermal-solar PV-fuel cell system.
- The study examines how the optimal placement of a TCSC and fuel cell in the proposed hybrid system can improve the system economy by curtailing the adverse effect of disequilibrium prices.
- The effect of FACTS devices and fuel cell placement on system voltage profiles and LBMP for the deregulated system has also been discussed in this paper.
- The study uses different optimization techniques such as Sequential Quadratic Programming (SQP) and Artificial Bee Colony Algorithms (ABC) to analyze the economic risk of the system.

This paper is categorized into different segments, each with a specific focus:

- **Segment I:** Focus on the background studies and the key features of this work.
- **Segment II:** Illustrates the mathematical approach implemented to validate the work presented.
- **Segment III:** Displays the objective functions along with the related constraints.
- **Segment IV:** Defines the preferred technique for evaluating system socioeconomic benefit in the deregulated power system.
- **Segment V:** Shows the results gained from the distinct segments through and beyond the incorporation of solar PV sources, fuel cells, and TCSC.
- **Segment VI:** Moreover, the study is carried out by incorporating a thyristor-controlled Series Compensator (TCSC)along with the fuel cell in the competitive power market. The practical solution is provided for power generators to increase their profits while simultaneously improving the stability and efficiency of the power grid. The outcomes of this work are shown in the last segment.

II. MATHEMATICAL MODELING

System modeling is a crucial step in the process of developing objectives, simulations, operations, and results. This paper has presented a hybrid model of solar-fuel cell-TCSC systems to create an objective function. In this section, all possible mathematical expressions of system parameters have been displayed.

A. SOLAR POWER

The mathematical equation that calculates the power generated by a photovoltaic (PV) array is as follows:

$$P = I_{pv} \times V \tag{1}$$

where, V = Supply voltage, I_{pv} = Photovoltaic current.

$$I_{pv} = n_p I_{ph} - n_p I_{sat}\left[e^{\frac{qF}{A_i kT}} - 1\right] - \frac{n_p F}{r_{sh}} \tag{2}$$

Here, the equations include several variables, including n_p, n_s, I_{ph}, I_{sat}, A_i, k, T, q, F, and r_{sh}.

$$F = \frac{V_{pv}}{n_s} + \frac{I_{pv} r_s}{n_p} \tag{3}$$

$$I_{ph} = \frac{S}{1000} [I_{sc} + k_i \{T - T_r\}] \tag{4}$$

$$I_{sat} = I_{rr} \left[\frac{T}{T_r}\right]^3 e^{\frac{qE_g}{A_i k}} \left[\frac{1}{T_r} - \frac{1}{T}\right] \tag{5}$$

n_p represents the number of PV cells connected in parallel, while n_s represents the number of cells connected in series. I_{ph} is the photocurrent generated by the PV array, and I_{sat} is the reverse saturation current. A_i, k, T, and q are the ideality factor, Boltzmann constant, cell absolute temperature, and electron charge respectively. F is an intermediate variable calculated using V_{pv} (photovoltaic voltage), n_s, I_{pv}, r_s (PV internal resistance in series), and n_p.

Equation (4) calculates the photocurrent (I_{ph}) of a solar cell based on the incident solar power (S), short-circuit current (I_{sc}), and temperature (T) of the cell. The term (S/1000) converts the incident solar power from watts per square meter to kilowatts per square meter. The term ($k_i \{T-T_r\}$) represents the temperature coefficient of the solar cell, where k_i is the short-circuit current temperature coefficient and T_r is the reference temperature. Equation (5) computes the saturation current (I_{sat}) of the solar cell based on the rated saturated current (I_{rr}), temperature (T), and energy band gap (E_g).

B. STATIC MODEL OF TCSC

A TCSC stands for Thyristor Controlled Series Compensator. It consists of a capacitor and an inductor connected to a couple of opposite-poled thyristors. By adjusting the firing angle of the thyristors, the inductor reactance can be varied, which changes the effective impedance of TCSC. Adding TCSC in series with the transmission line reduces the transfer reactance of that line connected between bus 'i' and bus 'j'.This reduction in transfer reactance increases the maximum power that can be transferred on that line and also reduces effective reactive power losses. The TCSC can be operated as capacitive or inductive compensation by directly modifying the reactance of the transmission line. The static model of TCSC is considered in the current work, and a variable reactance is connected in series to construct this model. The reactance of TCSC is a function of the reactance of the transmission line where TCSC is to be located as:

$$X_{Line} = X_{ij} + X_{TCSC} \tag{6}$$

$$X_{TCSC} = K_{TCSC} * X_{Line} \tag{7}$$

X_{Line} represents the total reactance of a transmission line. It is calculated by adding the reactance of the line itself (X_{ij}) and the reactance of the connected TCSC to the line (X_{TCSC}). The equation also introduces the variable (K_{TCSC}), which represents the compensation level of the TCSC. The reactance of the connected TCSC is calculated by multiplying the constant K_{TCSC} with the reactance of the line (X_{Line}).

The range of the compensation level of TCSC is limited to $-0.7 \leq K_{TCSC} \leq 0.2$. This means that the compensation level cannot exceed 20% of the reactance of the line, and it cannot be less than 70% of the reactance of the line.

C. FUEL CELL

The fuel cell model is a system that consists of an electrolyzer and a fuel cell. The electrolyzer uses the reverse reaction to electrolyze water and produce hydrogen. The fuel cell, on the other hand, converts the chemical energy of hydrogen into electrical energy. The reversible chemical interaction between oxygen and hydrogen produces electrical energy, heat, and water, as shown in the following equation:

$$2H_2 + O_2 \rightarrow H_2O + \text{Electrical Energy} + \text{Heat}$$

The generated hydrogen is stored in tanks for both short- and long-term storage. The efficiency of hydrogen storage is quite high compared to large-scale storage systems such as batteries or pumped hydro storage. There are two different operating periods in the system: low-demand and high-demand periods.

During the low-demand period, the electrolyzer produces hydrogen which is stored in tanks for later use.

The energy consumed by the electrolyzer (E_{elz}) is represented by the equation:

$$E_{elz} = \frac{hv^l_{H_2} \times E^p_{H_2}}{\eta_{elz}} \tag{8}$$

Here, $E^p_{H_2}$ represents the hydrogen produced by the electrolyzer, η_{elz} the efficiency of the electrolyzer, and $hv^l_{H_2}$ represents the lower heating value of hydrogen.

During the high-demand period, the stored hydrogen is used in the fuel cell to produce electricity. The energy produced by the fuel cell (E_{fc}) is represented by the equation:

$$E_{fc} = \eta_{fc} \times fc^{con}_{H_2} \times hv^l_{H_2} \tag{9}$$

Here, $fc^{con}_{H_2}$ represents the hydrogen consumption in the fuel cell, and η_{fc} represents the efficiency of the fuel cell.

D. LOCATION-BASED MARGINAL PRICE (LBMP)

Location-based Marginal Price (LBMP) is a method used in electricity markets to determine the price of electricity at specific locations in the grid. It considers the cost of transmitting electricity from the generation source to the location where it is consumed, as well as other factors such as demand and available generation capacity. With this method, the market clearing price for several nodes, or locations on a transmission grid is established. The marginal price at a node is essentially the sum of the variable cost of supply, transmission losses, and system congestion. In a typical LBMP system, the price of electricity is determined separately for each location in the grid, based on the cost of delivering electricity to that location. This can lead to different prices for electricity in different parts of the grid, even if they are supplied by the same power plant.

LMP is used in many electricity markets around the world, including in the United States, Europe, and Australia. It is an effective way to promote efficient use of the grid and to encourage investment in new transmission infrastructure.

E. SEQUENTIAL QUADRATIC PROGRAMMING (SQP)

The sequential quadratic programming (SQP) iterative approach has been used for solving the constrained non-linear problem. The mathematical issues where objective function and limitations are twice continuously differentiable can be resolved using SQP techniques. The SQP techniques are utilized in well-known numerical settings such as MATLAB and GNU Octave. The algorithm known as Sequential Quadratic Programming (SQP) is among the most used ones. It has strong theoretical underpinnings and a wide range of algorithmic capabilities.

F. ARTIFICIAL BEE COLONY (ABC) ALGORITHM

The Artificial Bee Colony (ABC) algorithm is an intelligence algorithm proposed by Karaboga in 2005, inspired by the activities of honey bees [28].

The algorithm uses a swarm of three types of bees: employed bees, onlooker bees, and scout bees. The employed bees search for sources of food from a pre-specified food source and share information about the food with the onlooker bees. The onlooker bees select the best quality food source based on the information shared by the employed bees. The scout bees are part of the employed bees and search for new quality food sources.

The step-by-step process of the Artificial Bee Colony (ABC) algorithm is as follows:

- The ABC algorithm is a meta-heuristic optimization algorithm inspired by the foraging behavior of honeybees.
- The algorithm starts with initializing the population and other system variables.
- The employed bee phase is then defined and started, where each employed bee searches for a food source in the search space.
- The onlooker bee phase is then defined and started, where each onlooker bee chooses a food source based on the information shared by the employed bees.
- The source position of the best food is checked and stored.
- The availability of scout bees in the colony is checked. If there are scout bees, the scout bee phase is started, where each scout bee searches for a new food source.
- The algorithm checks for the meeting of termination criteria. If the criteria are met, the algorithm proceeds to the next step. Otherwise, it goes back to the employed bee phase.
- Finally, the best solution is obtained.

III. OBJECTIVE FUNCTION

In a regulated power market, there was limited transparency in economic aspects between GENCOS and customers. This lack of transparency may benefit GENCOS, but customers suffer. Deregulation was introduced to enhance customer benefits by creating competition among market players such as GENCOS, TRANSCOS (transmission companies), DISCOS (distribution companies), and retailers. Due to increased transparency and competition, customers benefit from the deregulated power market (i.e. social benefit). ISO (Independent System Operator) plays an important role in this scenario by controlling the electricity market. ISO collects bids from GENCOS and DISCOS and performs optimization to fix the location-based marginal price (LBMP). The day-ahead market is an important aspect of the competitive power market that provides economic benefits to society. In the renewable associated day-ahead market, GENCOS needs to submit details about future power generation to the ISO. While thermal power plants do not face any issues in this market, renewable power plants face problems due to the uncertain nature of power generation. If there is a mismatch between expected and real solar power generation, ISO imposes penalties or rewards on the solar plant for their shortfall or extra power supply. This is known as the disequilibrium price.

This work aims to maximize the profit of the solar-integrated deregulated electrical system, but the negative impact of disequilibrium price can reduce this profit. To minimize the adverse effect of disequilibrium prices, a methodology has been proposed to optimize the operation of solar PV systems along with the fuel cell and TCSC. The fuel cell operates as a backup source to provide additional generated energy to minimize the mismatch between expected and real solar energy. The fuel cell compensates for the lower amount of energy generated from the solar plant and tries to maintain the contracts signed between GENCOS and ISO. The methodology proposed in this work has been implemented using Sequential Quadratic Programming (SQP).

A test system is been considered with the number of buses as 'N_{BUS}', power transmission lines as 'N_{PTL}', load demands as 'N_{LD}', and generators as 'N_G'. The study aims to integrate TCSC and fuel cells into a renewable incorporated deregulated system efficiently to maximize social benefit and revenue while reducing generation expenses and system economic risk in the context of disequilibrium prices. The disequilibrium prices must be considered for any operational study related to a renewable incorporated system. The positive disequilibrium price provides enhanced profit to the system while the adverse disequilibrium price delivers minimal profit. This outcome is observed due to the grid operators' simultaneous application of incentives and sanctions to GENCOs. The main objective of this work is to enhance the system's profit and reduction of economic risk. The objective functions are as follows:

$$P_{MAX}(i,t) = R_T(i,t) + DP(i,t) - GC_T(i,t) \tag{10}$$

Here, the objective is to maximize the overall profit at a given time 't' in the *i*-th unit, denoted by $P_{MAX}(i,t)$. This profit is the generator company's profit. So, after the implementation of renewable integration, these values will be maximized but, this will reduce when the system is converted from regulated to deregulated. The overall profit is a function of three variables: total revenue denoted by R_T(i,t), disequilibrium price denoted by DP(i,t), and the overall generation cost (including both thermal- and wind generation) denoted by GC_T(i,t).

$$R_T(i,t) = \sum_{i=1}^{N} P_R(i,t).LBMP(i,t) \tag{11}$$

$$DP(i,t) = \sum_{i=1}^{N} ((EC(i,t) + SC(i,t)\frac{P_E(i,t)}{P_R(i,t)}).^2) \cdot (P_R(i,t) - P_E(i,t)) \tag{12}$$

Equation (11) & (12) shows the total revenue and the disequilibrium price calculation. Where P_R is the real and P_E is the expected power generated from the solar power plant at the given time 't'. The shortfall charge rate is denoted by SC and the extracharge rate is shown by EC. The disequilibrium price is calculated by summing up the product of the charge rates and the difference between the real and expected power output. The disequilibrium price is caused by the discrepancy between expected and real solar irradiance and temperature in a solar-integrated system. The disequilibrium price directly affects the system economy in a competitive power network.

$$GC_T(i,t) = GC_{Ther}(i,t) + GC_{solar}(i,t) + IC_{TCSC} \tag{13}$$

Equation (13) shows the total generation cost of the system by adding the generation costs of conventional and solar power sources at a specific bus and time, along with the cost of the TCSC used in the system. Here GC_T (i,t) represents the total generation cost of the system at the bus-n and time 't'. GC_{Ther}(i,t) represents the generation cost of the conventional power sources (i.e. thermal). GCsolar(i,t) represents the generation cost of the solar power sources. IC_{TCSC} represents the investment cost of the TCSC used in the system.

$$GC(i,t) = \sum_{i=1}^{N} (a_i + b_i P_R(i,t) + C_i P_R^2(i,t)) \tag{14}$$

Equation (14) presents GC(i,t) as the generation cost of the n-th generator at time t. a_i, b_i, and C_i are the coefficients of the quadratic cost function for the n-th generator. When real solar power (RSP) differs from expected solar power (ESP), the fuel cell can be used to reduce the power disparity and make up for the discrepancy.

$$SC(i,t) = (1+\beta).LBMP(i,t), EC = 0; \quad \text{if } P_E(i,t) > P_R(i,t) \tag{15}$$

$$EC(i,t) = (1-\beta).LBMP(i,t), SC = 0; \quad \text{if } P_E(i,t) < P_R(i,t) \tag{16}$$

$$EC(i,t) = SC(i,t) = 0; \quad \text{if } P_E(i,t) = P_R(i,t) \tag{17}$$

where 'λ' is the disequilibrium price coefficient. Equation (15), (16), and (17) shows the relationship between shortfall and extra charge rate while considering the expected and real solar irradiance and temperature. It varies between 0 to 1. A value of 0.9 is considered in this work.

A. OPERATING CONSTRAINTS FOR FUEL CEL

A fuel cell is an energy storage device that utilizes the energy obtained from hydrogen. It produces clean and efficient electricity. During low power demand time, the excess energy is utilized by the electrolyzer for generating the molar of hydrogen which can be stored in a hydrogen reservoir. And during the deficit of power in the grid, the stored power can be utilized to fulfill the need. The minimum and maximum constraints for the electrolyzer's power consumption are discussed below:

$$PC_{ELZ}^{Min} \le PC_{ELZ} \le PC_{ELZ}^{Max} \tag{18}$$

Additionally, the following provides the electrolyzer's hydrogen production constraint:

$$H_2^{Min}{}_{ELZ} \le H_2.{}_{ELZ} \le H_2^{Max}{}_{ELZ} \tag{19}$$

Moreover, the hydrogen that is being stored produces electricity to satisfy peak demand when the system is in fuel cell mode. Therefore, the limitations are listed:

$$P_{Gen}^{FC\_Min} \le P_{Gen}^{FC} \le P_{Gen}^{FC\_Max} \tag{20}$$

$$H_2^{Min}{}_{FC\_CONS} \le H_2.{}_{FC\_CONS} \le H_2^{Max}{}_{FC\_CONS} \tag{21}$$

Therefore, The constraint ensures that the fuel cell operates within a certain range of energy output, which is necessary for the optimal operation of the hybrid system. The constraint on the consumption of hydrogen in the fuel cell system is important to ensure the optimal operation of the system and to prevent any damage to the system components.

B. CONSTRAINTS FOR SOLVING OPTIMAL POWER FLOW

To solve the OPF problem, equality, and inequality constraints have been considered.

1) EQUALITY CONSTRAINTS

Equality Constraints refer to a set of nonlinear equations that must be satisfied simultaneously in a system.

In this case, the equality constraints are used to ensure that the real power is balanced in the system. The equation for real power balance is given by:

$$\sum_{i=1}^{N_G} P_{gi} - P_{loss} - P_L = 0 \tag{22}$$

where P_{gi} is the real power generated by the i^{th} generator, P_{loss} is the real power exported to the grid by the system, and P_L is the real power consumed by the loads in the system.

$$P_{loss} = \sum_{j=1}^{N_{PTL}} G_J \left[|V_i|^2 + |V_j|^2 - 2|V_i||V_j|\cos(\delta_i - \delta_j) \right] \tag{23}$$

Equation (23) is used to calculate the power losses in the system. Where P_{loss} is the power loss in the system, G_J is the conductance of the j^{th} transmission line, and V_i and V_j are the voltage magnitudes at the sending and receiving ends of the j^{th} transmission line. δ_i and δ_j are the voltage phase angles at the sending and receiving ends of the j[th] transmission line, respectively.

$$P_i \sum\nolimits_{K=1}^{N_{BUS}} |V_i V_K Y_{ik}| \cos(\theta_{iK} - \delta_i - \delta_k) = 0 \quad (24)$$

$$Q_i + \sum\nolimits_{K=1}^{N_{BUS}} |V_i V_K Y_{ik}| \sin(\theta_{iK} - \delta_i - \delta_k) = 0 \quad (25)$$

Equation (24) calculates the active power flow from bus-i to all other buses in the system. V_i is the voltage magnitude at bus i, V_k is the voltage magnitude at bus k, Y_{ik} is the admittance between buses i and k. θ_{iK} is the phase angle difference between bus i and k. δ_i and δ_k are the voltage phase angles at buses i and k respectively. The Cos function calculates the cosine of the phase angle difference between bus i and k, which determines the direction of active power flow. Equation (25) calculates the reactive power flow at bus i. Q_i is the reactive power injection or absorption at bus-i. The Sin function calculates the sine of the phase angle difference between buses i and k plus the reactive power injection or absorption at bus k, which determines the direction of reactive power flow.

2) IN-EQUALITY CONSTRAINTS

$$P_{gi}^{min} \le P_{gi} \le P_{gi}^{max} \quad i = 1, 2, 3 \ldots\ldots N_{BUS} \quad (26)$$

$$Q_{gi}^{min} \le Q_{gi} \le Q_{gi}^{max} \quad i = 1, 2, 3 \ldots\ldots N_{BUS} \quad (27)$$

$$V_i^{min} \le V_i \le V_i^{max} \quad i = 1, 2, 3 \ldots\ldots N_{BUS} \quad (28)$$

$$\phi_i^{min} \le \phi_i \le \phi_i^{max} \quad i = 1, 2, 3 \ldots\ldots N_{BUS} \quad (29)$$

$$TL_l \le TL_l^{max} \quad i = 1, 2, 3 \ldots\ldots N_{PTL} \quad (30)$$

Here, P_{gi}^{min} and P_{gi}^{max} represent the minimum and maximum real power respectively, that can be generated at the PV bus-a. Q_{gi}^{min} and Q_{gi}^{max} represent the minimum and maximum reactive power respectively. P_{gi} and Q_{gi} represent the real and reactive power. The inequalities present in (26) and (27) ensure that the real and reactive power generated at the PV bus remains within the specified limits. V_i^{min} and V_i^{max} represent the minimum and maximum voltage magnitudes respectively. The inequality $V_i^{min} \le V_i \le V_i^{max}$ ensures that the voltage magnitude at the PQ bus remains within the specified limits. ϕ_i^{min} and ϕ_i^{max} represent the minimum and maximum phase angles respectively, that can be maintained at the PQ bus. TL_l^{max} represents the maximum transmission capacity of the connected line that connects the line TL_l.

C. CONSTRAINTS FOR TCSC

$$K_{TCSC}^{min} \le K_{TCSC} \le K_{TCSC}^{max} \quad (31)$$

Equation (31) refers to a constraint on the value of a variable called K_{TCSC}. This variable represents the control parameter of a TCSC. The symbols 'min' and 'max' denote the minimum and maximum values of K_{TCSC} respectively. Therefore, the constraint states that the value of This constraint is part of an optimization approach proposed in the paper to optimally allocate TCSC and other devices in a power system with a solar generator under deregulated conditions.

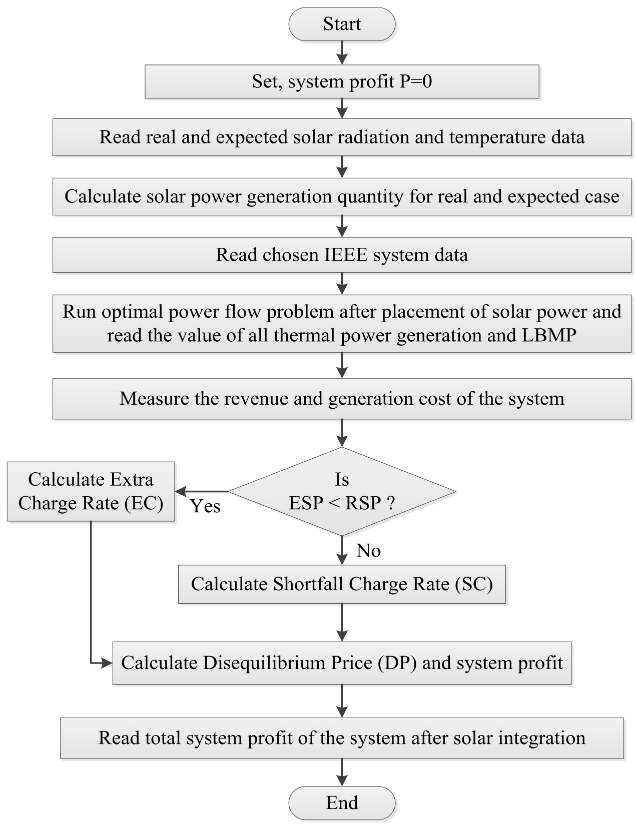

FIGURE 1. Flow-chart for disequilibrium price calculation.

IV. FLOW CHART OF THE PROPOSED TECHNIQUES

This section displays the flow charts of the proposed method. Fig. 1 shows the process involved in calculations of the system disequilibrium price and system profit.

TCSC is a device used in power systems to control the flow of power by adjusting the impedance of transmission lines. Fig. 2 displays the method to optimally allocate TCSCs in a power system. The algorithm places a TCSC in every line of the system and calculates the objective for each case. The objective function is a mathematical expression representing the optimization problem's goal. In this case, the objective function is to minimize the generation cost of the power system. Finally, the algorithm selects the lines with minimum objective function and places the TCSCs in those lines.

V. RESULTS AND DISCUSSIONS

A modified IEEE 14-bus test system has been chosen to validate the presented approach. The IEEE 14-bus system consists of 14 interconnected buses using 20 transmission lines, 5 generator buses, and 9 load buses. Bus no. 1 was designated as the slack bus and the system MVA limit was set to 100 MVA. The modified IEEE 14-bus test system was adapted from references [29] and is shown in Fig. 3.

The step-by-step process for implementing the presented work is as:

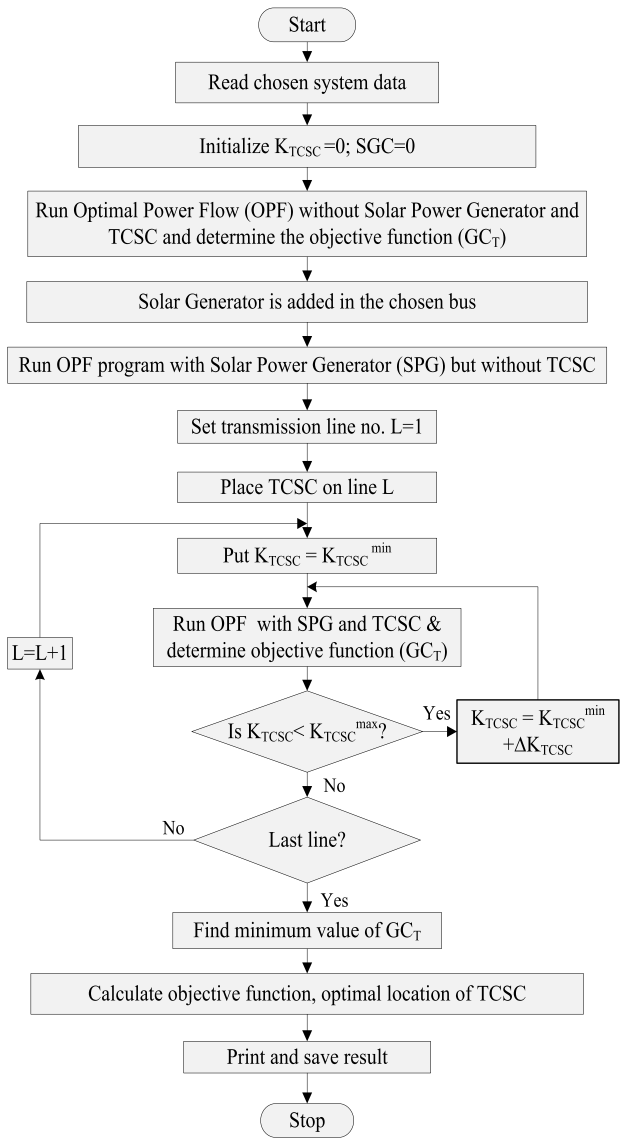

FIGURE 2. Flow-chart for optimal placement of TCSC.

- ***Step 1: Data Collection-*** Read all system information for the considered test system. This step involves gathering all the necessary information about the power system being considered for the study.
- ***Step 2: Scenario Generation-***Generate different scenarios for verifying the applicability of the proposed method. These scenarios are created on a random basis.
- ***Step 3: Economic Parameter Measurement with Random Data-***This step involves calculating the system generation cost, revenue, and profit for both with and without considering solar generation in the system. A comparative study of system economic parameters has been performed for regulated and deregulated systems.
- ***Step 4: Economic Parameter Measurement with Real-time Data-*** The process of step- 3 is repeated here by considering the real-time solar power data.
- ***Step 5: Optimal TCSC Placement-*** Checking for the optimal placement of TCSC. After that, place the TCSC in the optimal location and perform all the economy-related comparative studies.
- ***Step 6: Calculation of Disequilibrium Price-*** Calculate the disequilibrium price considering real and expected solar radiation and temperature data and compare the system profit with and without the disequilibrium price for the deregulated system.
- ***Step 7: Fuel Cell Placement-*** Place the fuel cell in the considered system and check the system's profit.
- ***Step 8: Comparison of Profit with Different Optimization Techniques-*** Compare the system economy with different optimization techniques.

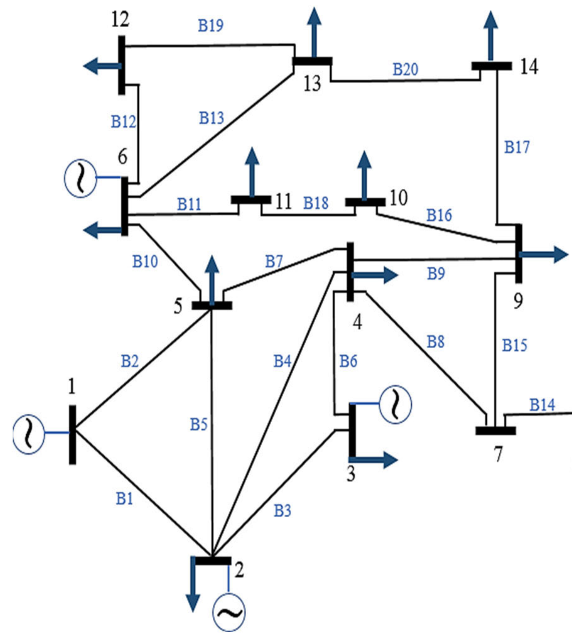

FIGURE 3. Single line diagram of IEEE 14 bus system.

A. STEP 1: DATA COLLECTION

The basic system parameters of the selected system are shown in Table 1. In Table 1, P_d represents active power demand, Q_d represents reactive power demand, V_m represents voltage magnitude and V_a represents voltage angle. Vmax and Vmin are maximum and minimum voltages respectively.

The system profit depends on the revenue earned by the generation stations and the cost involved in generating the power. Due to the limited availability of coal, the electrical sectors are moving towards the renewable-dominated grid. The regulated to deregulated power system transformation has only been performed to benefit the consumer in terms of the electrical economy as well as for the quality of the electricity. In this work, the optimal power flow has been solved for all the considered cases to get the system revenue, system generation cost, and profit in a regulated and deregulated environment.

B. STEP 2: SCENARIO GENERATION

Solar power generation depends on two environmental parameters: solar radiation/irradiance and temperature.

TABLE 1. Basic parameters of IEEE 14-bus system.

Bus No.	Pd	Qd	Vm	Va	Vmax	Vmin
1	0	0	1.06	0	1.06	0.94
2	21.7	12.7	1.045	-4.98	1.06	0.94
3	94.2	19	1.01	-12.72	1.06	0.94
4	47.8	-3.9	1.019	-10.33	1.06	0.94
5	7.6	1.6	1.02	-8.78	1.06	0.94
6	11.2	7.5	1.07	-14.22	1.06	0.94
7	0	0	1.062	-13.37	1.06	0.94
8	0	0	1.09	-13.36	1.06	0.94
9	29.5	16.6	1.056	-14.94	1.06	0.94
10	9	5.8	1.051	-15.1	1.06	0.94
11	3.5	1.8	1.057	-14.79	1.06	0.94
12	6.1	1.6	1.055	-15.07	1.06	0.94
13	13.5	5.8	1.05	-15.16	1.06	0.94
14	14.9	5	1.036	-16.04	1.06	0.94

TABLE 2. Considered case details.

Case No.	Description
Base case	Solar power is not placed in the system
Case 1	Solar power of 3MW is placed at bus 4
Case 2	Solar power of 5MW is placed at bus 4
Case 3	Solar power of 3MW is placed at bus 9
Case 4	Solar power of 5MW is placed at bus 9
Case 5	Solar power of 3MW is placed at bus 11
Case 6	Solar power of 5MW is placed at bus 11
Case 7	Solar power of 3MW is placed at bus 14
Case 8	Solar power of 5MW is placed at bus 14

TABLE 3. Profit for the regulated system (In $/h).

Case No.	Generation Cost			Revenue			Profit
	Thermal	Solar	Total	Thermal	Solar	Total	
Base case	8081.53	0	8081.53	10052.32	0	10052.32	1970.79
Case 1	7961.02	22.875	7983.895	9924.832	120.438	10045.27	2061.37
Case 2	7880.76	38.125	7918.885	9840.27	200.585	10040.85	2121.97
Case 3	7961.1	22.875	7983.975	9925.92	120.36	10046.28	2062.3
Case 4	7880.89	38.125	7919.015	9842.453	200.445	10042.89	2123.88
Case 5	7961.31	22.875	7984.185	9924.303	119.973	10044.27	2060.09
Case 6	7841.58	38.125	7879.705	9796.648	199.145	9995.79	2116.08
Case 7	7958.3	22.875	7981.175	9922.291	122.868	10045.15	2063.98
Case 8	7876.54	38.125	7914.665	9835.368	203.985	10039.35	2124.68

TABLE 4. Profit for the deregulated system(In $/h).

Case No.	Generation cost			Revenue			Profit
	Thermal	Solar	Total	Thermal	Solar	Total	
Base case	7538.06	0	7538.06	9467.63	0	9467.63	1929.57
Case 1	7418.2	22.87	7441.07	9339.55	119.76	9459.31	2018.24
Case 2	7338.42	38.12	7376.54	9248.57	199.24	9447.81	2071.27
Case 3	7417.97	22.87	7440.84	9339.23	119.96	9459.19	2018.35
Case 4	7338.07	38.12	7376.19	9248.01	199.51	9447.52	2071.33
Case 5	7418.63	22.87	7441.5	9339.09	119.15	9458.24	2016.74
Case 6	7299.8	38.12	7337.92	9203.53	197.5	9401.03	2063.11
Case 7	7416.14	22.87	7439.01	9335.86	121.51	9457.37	2018.36
Case 8	7335.33	38.12	7373.45	9244.28	201.54	9445.82	2072.37

Considering the variable nature of solar irradiance and solar cell temperature, several scenarios have been developed in this part of the work to check the efficacy of the modeled methods. The details about the considered cases are shown in Table 2. The investment cost of solar energy is approximately 7.625 $/MWh, which was collected from different works of literature and case studies.

For the first considered case (i.e. base case), the solar PV has not been placed whereas for the other cases, solar PV has been installed at busno. 4, 9, 11, and 14 with a generating capacity of 3MW and 5MW respectively. The placement of solar PV and the capacity of the solar power have been considered as random selection.

C. STEP 3: ECONOMIC PARAMETER MEASUREMENT WITH RANDOM DATA

Referring to the equation of the profit in equation 10, generation cost and revenue for both thermal and solar are calculated. The total system profit is calculated from the total generation cost and total revenue. The system profit is calculated for both regulated and deregulated systems. Converting from a regulated to a deregulated environment, the demand bus bidding is provided from bus no. 5. Table 3 and Table 4 refer to the profit for the regulated and deregulated system respectively. From Table 3 and Table 4, it is seen that the system profit is maximized with the placement of solar PV in the system. The maximum amount of solar PV placement maximizes the electricity producers' profit.

On the other side, it is also found that the system profit is reduced when converting from a regulated to a deregulated environment. The main objective of the deregulated system is to maximize the social benefit which indicates less benefit to the power producer. So, the profit measurement in the regulated and deregulated environment proves the main aim of the conversion of the power system. Like a regulated system, here also it is observed that the profit is maximized with the placement of solar power in the system.

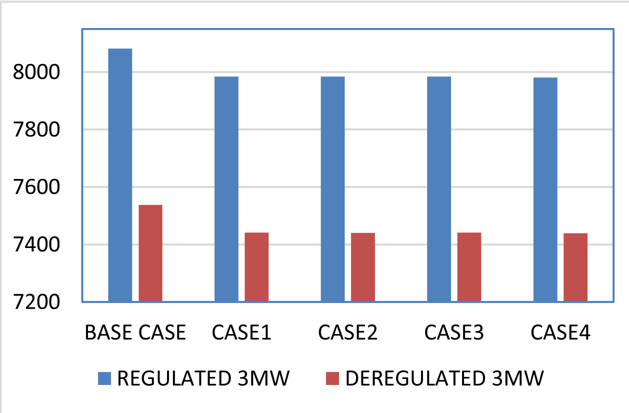

FIGURE 4. Generation cost for the placement of 3MW solar power capacity (In $/h).

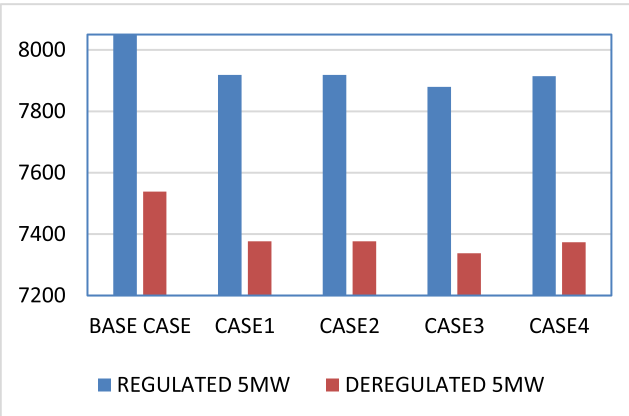

FIGURE 5. Generation cost for the placement of 5 MW solar power capacity (In $/h).

D. COMPARATIVE STUDIES

As part of this work, the generation cost is calculated and compared for both regulated and deregulated systems with four considered cases considering the placement of 3MW and 5MW of solar PV in the solar integrated system.

Table 5 and Fig. 4 display the comparison of generation cost for both regulated and deregulated systems with the incorporation of 3 MW solar power in the thermal power plant. In this section, only the first 4 scenarios along with the base case have been chosen to check the effect of the presented model. From the results, it is seen that the generation cost is reduced for every case when the system is converted to deregulation. It happens due to the huge competition in the electrical system regarding power generation. Table 6 and Fig. 5 show the comparative studies of system generation cost for different case studies with 5 MW solar energy integration in the system.

From the detailed study, it is observed that the system generation cost is reduced for both regulated and deregulated systems after the placement of solar power in the system. Like system generation cost, the same process is followed for the system revenue calculation and comparison has been performed for both regulated and deregulated systems with the four considered cases for 3MW and 5MW of solar energy installation. Table 7, Fig. 6, Table 8, and Fig. 7 depict the comparative studies of system revenue (earned by the power producer) for different case studies with different amounts of solar energy integration in the system.

Solar power placement is crucial in a regulated and deregulated system, as shown in Table 3 and Table 4. Integrating the maximum amount of solar power in the system leads to

TABLE 5. Generation cost for 3MW (In $/h).

	Base Case	Case 1	Case 2	Case 3	Case 4
Regulated 3 MW	8081.53	7983.90	7983.975	7984.185	7981.175
Deregulated 3MW	7538.06	7441.075	7440.845	7441.505	7439.015

TABLE 6. Generation cost for 5MW (In $/h).

	Base Case	Case 1	Case 2	Case 3	Case 4
Regulated 5 MW	8081.53	7918.885	7919.015	7879.705	7914.665
Deregulated 5 MW	7538.06	7376.545	7376.195	7337.925	7373.455

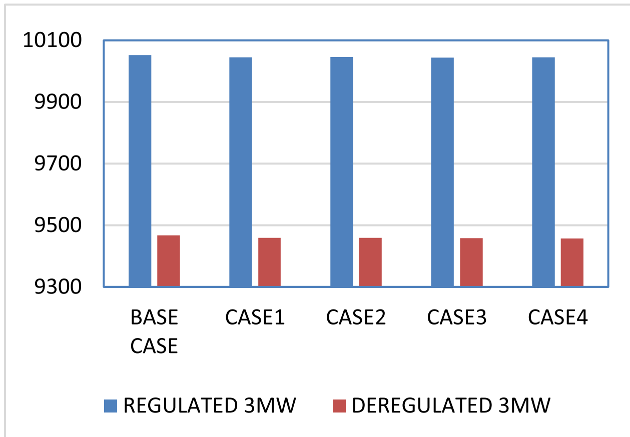

FIGURE 6. Revenue for the placement of 3 MW solar power capacity (In $/h).

TABLE 7. Revenue for 3MW(In $/h).

	Base Case	Case 1	Case 2	Case 3	Case 4
Regulated 3 MW	10052.32292	10045.27	10046.28	10044.28	10045.1595
Deregulated 3 MW	9467.63819	9459.316	9459.191	9458.249	9457.37878

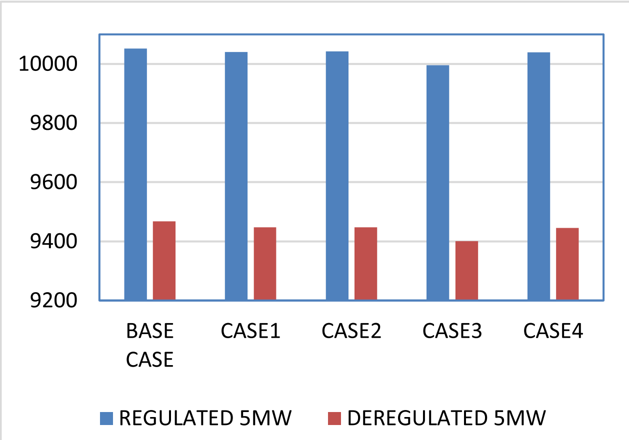

FIGURE 7. Revenue for the placement of 5 MW solar power capacity (In $/h).

TABLE 8. Revenue for 5 MW (In $/h).

	Base Case	Case 1	Case 2	Case 3	Case 4
Regulated 5 MW	10052.32292	10040.85	10042.898	9995.793	10039.35
Deregulated 5 MW	9467.63819	9447.818	9447.52646	9401.036	9445.824

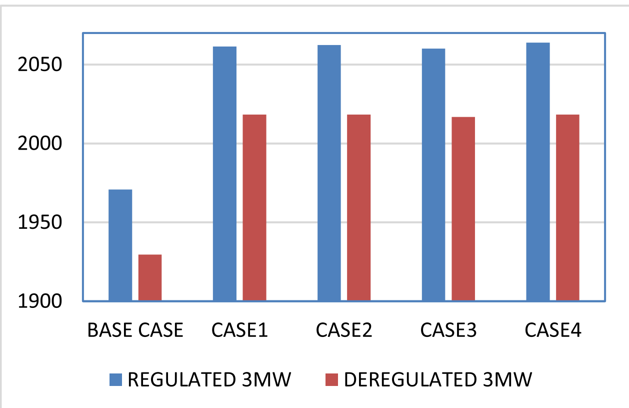

FIGURE 8. Profit for the placement of 3 MW solar power capacity(In $/h).

minimum system generation costs. Solar PV placement also affects the supplier's profit, with maximum profit achieved by placing high-value solar power and minimum profit without implementing a solar power integration in the system. From the system revenue and system generation cost, the system profit has been measured. This system's profit is displayed as the profit of the power producers. So, it is obvious that the value of system profit will reduce after the conversion of the system to a deregulated environment. The highest amount of solar power integration leads to the most economic result for the solar-associated deregulated power system. Table 9, Fig. 8, Table 10, and Fig. 9 depict the comparative studies of system profit for different case studies with different amounts of solar energy integration in the system.

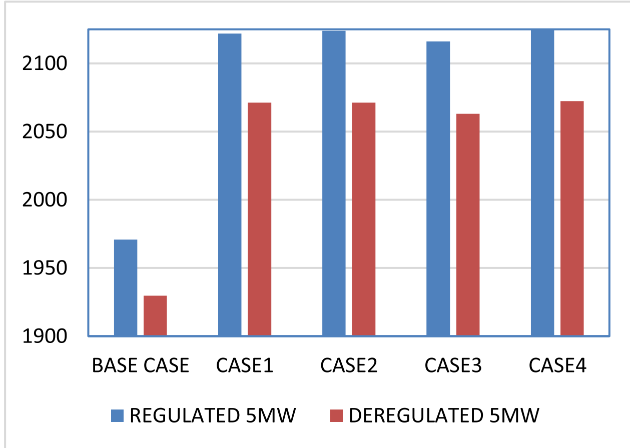

FIGURE 9. Profit for the placement of 5 MW solar power capacity(In $/h).

TABLE 9. Profit for 3 MW(In $/h).

	Base Case	Case 1	Case 2	Case 3	Case 4
Regulated 3 MW	1970.79	2061.37	2062.3	2060.09	2063.98
Deregulated 3 MW	1929.58	2018.24	2018.35	2016.74	2018.36

TABLE 10. Profit for 5 MW(In $/h).

	Base Case	Case 1	Case 2	Case 3	Case 4
Regulated 5 MW	1970.79	2121.96	2123.88	2116.08	2124.68
Deregulated 5 MW	1929.58	2071.27	2071.33	2063.11	2072.37

The profit comparison with and without placement of solar power at bus no. 4, 9, 11, and 14 are plotted for both regulated and deregulated systems and are shown in Fig. 10. From the results it can be concluded that the solar power integration provides the maximum profit to the power producer as compared to the without solar installation scenarios.

However, the profit is changing with changing the position of the solar PV installation. It is seen that the system profit gets maximum when the solar power is installed at bus no. 14 of the considered system. So, it can be said that the optimal position of solar placement is at bus no. 14 of the selected IEEE 14-bus system. Considering the flexible nature of solar power generation, here two different quantities of solar power have been applied to check the feasibility of the presented method.

E. STEP 4:ECONOMIC PARAMETER MEASUREMENT WITH REAL-TIME DATA

Solar irradiance varies in every period throughout the world, making it a flexible energy source. The study considers one place in India, Vijayawada, for real-time problem-solving. The solar irradiance and temperature have been collected for

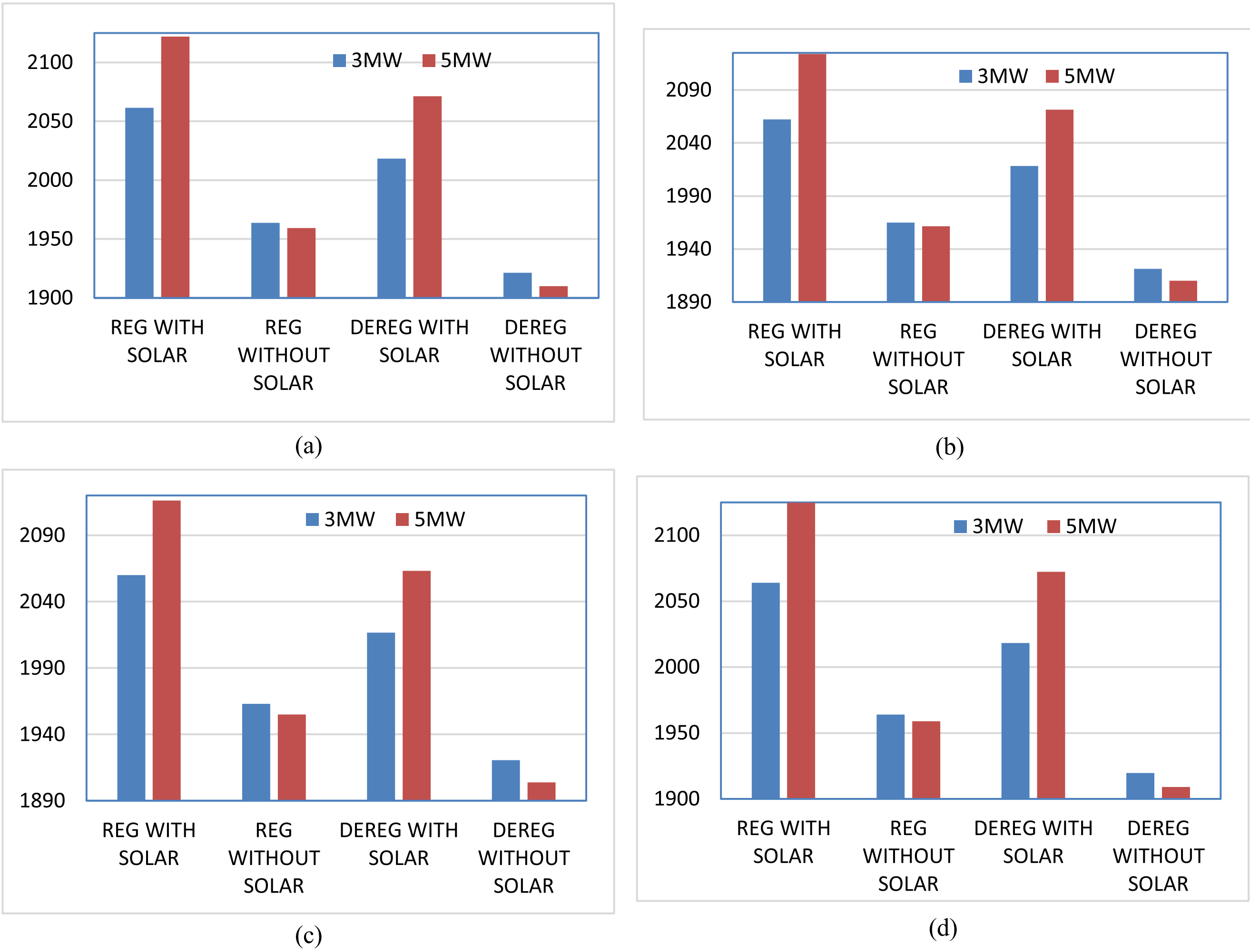

FIGURE 10. **Profit comparison at Bus 4, 9, 11, 14(In $/h).**

TABLE 11. **Real-time solar power data (In MW).**

Hour	**1**	**2**	**3**	**4**	**5**	**6**	**7**	**8**
Solar Power	0	0	0	0	0	0	0.09	0.55
Hour	**9**	**10**	**11**	**12**	**13**	**14**	**15**	**16**
Solar Power	0.68	0.67	1.01	1.68	1.63	1.54	1.84	1.7
Hour	**17**	**18**	**19**	**20**	**21**	**22**	**23**	**24**
Solar Power	0.45	0.29	0.02	0	0	0	0	0

24-hour cases for considered places. Using equations 1-5, the solar power generation capacity has been measured for every hour of the selected day, shown in Table 11.

The running cost or generation cost of solar power is zero, only the investment cost is present for the solar plant. The approximate solar power investment cost is 7.625 $/MWh which has been considered here for the economic performance of the solar plant. Table 12 depicts the considered case details for real-time data in an electrical system. The table consists of solar power data generated by a renewable energy source for every hour of the day. A total of 13 cases along with base cases have been considered here because other periods not generating any solar power. For the first considered case (i.e. base case), the solar PV has not been placed whereas, for the other cases, solar PV has been installed at bus no. 4 with the generating capacity of 0.09 MW, 0.44 MW, 0.68 MW, 0.67 MW, 1.01 MW, 1.68 MW, 1.63 MW, 1.53 MW, 1.84 MW, 1.70 MW, 0.45 MW, 0.29 MW, and 0.02 MW respectively (neglecting the night time data).

The placement of solar PV has been considered a random selection. Referring to the equation of the system profit; generation cost and Revenue for both thermal and solar power are calculated. The total profit is calculated from the total generation cost and total revenue. Here, the total economic parameter is considered with the combination of thermal and solar power. Similar to the previous section, profit is calculated here for the regulated and deregulated systems by considering the real-time scenarios. Table 13 and Table 14 refer to the profit for the regulated and deregulated system based on real-time data respectively. From the Tables,

TABLE 12. Considered case details for real-time data.

Case No.	Hour	Description
Base case	---	Solar power is not placed at any of the buses
Case 1	7th Hour	Solar power of 0.09 MW is placed at bus 4
Case 2	8th Hour	Solar power of 0.44 MW is placed at bus 4
Case 3	9th Hour	Solar power of 0.68 MW is placed at bus 4
Case 4	10th Hour	Solar power of 0.67 MW is placed at bus 4
Case 5	11th Hour	Solar power of 1.01 MW is placed at bus 4
Case 6	12th Hour	Solar power of 1.68 MW is placed at bus 4
Case 7	13th Hour	Solar power of 1.63 MW is placed at bus 4
Case 8	14th Hour	Solar power of 1.54 MW is placed at bus 4
Case 9	15th Hour	Solar power of 1.84 MW is placed at bus 4
Case 10	16th Hour	Solar power of 1.70 MW is placed at bus 4
Case 11	17th Hour	Solar power of 0.45 MW is placed at bus 4
Case 12	18th Hour	Solar power of 0.29 MW is placed at bus 4
Case 13	19th Hour	Solar power of 0.02 MW is placed at bus 4

TABLE 13. Profit for the regulated system based on real-time data(In $/h).

Case No.	Revenue		Generation cost		Profit
	Thermal	Solar	Thermal	Solar	
Base case	10052.32	0	8081.53	0	1970.793
Case 1	10048.87	3.61701	8077.91	0.68625	1973.888
Case 2	10034.07	17.68096	8063.84	3.355	1984.555
Case 3	10023.99	27.3224	8054.2	5.185	1991.927
Case 4	10024.4	26.9206	8054.6	5.10875	1991.612
Case 5	10009.64	40.57675	8040.94	7.70125	2001.576
Case 6	9981.344	67.47888	8014.03	12.81	2021.983
Case 7	9982.998	65.47058	8016.03	12.42875	2020.01
Case 8	9986.828	61.85872	8019.65	11.7425	2017.294
Case 9	9974.315	73.89992	8007.6	14.03	2026.585
Case 10	9980.508	68.2805	8013.22	12.9625	2022.606
Case 11	10033.29	18.0828	8063.44	3.43125	1984.502
Case 12	10043.82	11.65423	8073.09	2.21125	1980.171
Case 13	10051.88	0.8038	8080.72	0.1525	1971.811

it has been seen that the system profit is maximized with the placement of solar PV in the system. The maximum amount of solar PV placement maximizes the electricity producers' profit. i From the data, it has been seen that maximum solar power occurred at hour-15 (i.e. case-9) and minimum solar power occurred at hour-19 (i.e. case-13) which also indicates the economic sustainability of the solar-integrated system. When the entire world is thinking about the conversion to

TABLE 14. Profit for the deregulated system based on real-time data(In $/h).

Case No.	Revenue		Generation cost		Profit
	Thermal	Solar	Thermal	Solar	
Base case	9467.638	0	7538.06	0	1929.578
Case 1	9463.801	3.59784	7534.46	0.68625	1932.252
Case 2	9448.565	17.5868	7520.47	3.355	1942.326
Case 3	9438.505	27.17688	7510.88	5.185	1949.617
Case 4	9439.31	26.77722	7511.28	5.10875	1949.699
Case 5	9424.413	40.3596	7497.69	7.70125	1959.381
Case 6	9395.845	67.11096	7470.92	12.81	1979.226
Case 7	9397.708	65.11524	7472.92	12.42875	1977.474
Case 8	9401.864	61.523	7476.51	11.7425	1975.135
Case 9	9389.033	73.49512	7464.53	14.03	1983.968
Case 10	9394.675	67.9082	7470.12	12.9625	1979.501
Case 11	9448.128	17.9865	7520.07	3.43125	1942.613
Case 12	9458.784	11.59246	7529.67	2.21125	1938.495
Case 13	9466.832	0.79954	7537.26	0.1525	1930.219

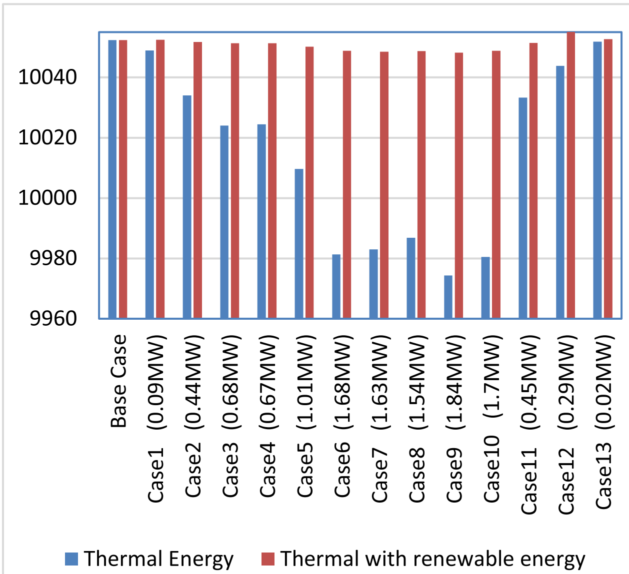

FIGURE 11. Revenue comparison for regulated system (In $/h).

renewable-associated systems, this result encourages electrical energy providers to invest their money in solar farms. All the economic parameters i.e. revenue, generation cost, and profit comparison with and without placement of solar power in regulated systems are shown in Fig. 11, Fig. 12, and Fig. 13 respectively. All the results depict the economic advancement of the system with solar power installation.

Location-based Marginal Pricing (LBMP) for the IEEE 14-bus system in a regulated system is calculated to measure the cost of delivering electricity at different locations in the

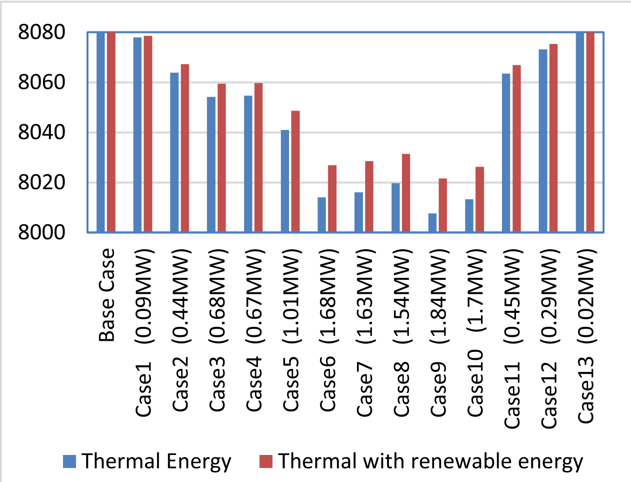

FIGURE 12. **Generation cost comparison for regulated system (In $/h).**

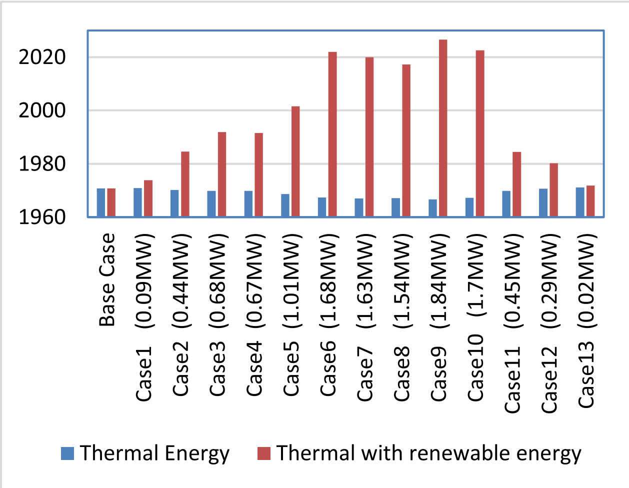

FIGURE 13. **Profit comparison for regulated system (In $/h).**

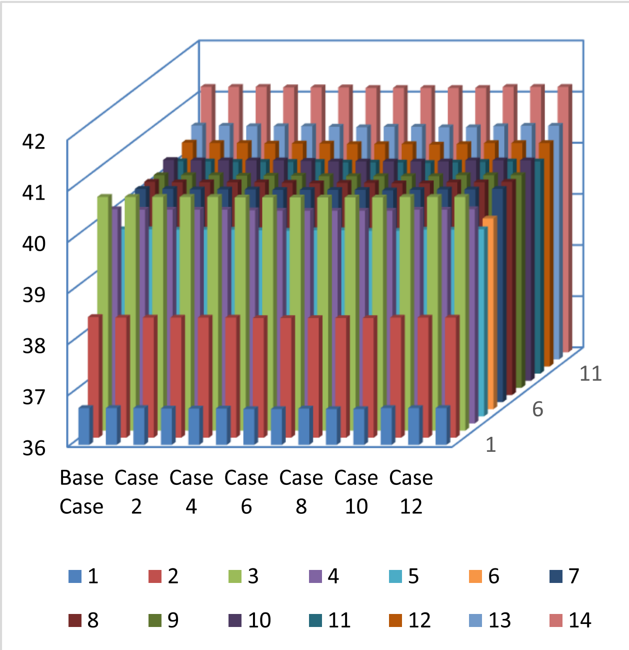

FIGURE 14. **LBMP for IEEE14 bus system for regulated system (In $/MWh).**

power system. LBMP is a market-based mechanism used in electricity markets to determine the price of electricity at different locations in the power system. LBMP is calculated by taking into account the costs of generating, transmitting, and distributing electricity to different locations in the power system. The LBMP at a specific location reflects the marginal cost of supplying an additional unit of electricity at that location. By calculating LBMP at different locations in the power system, market participants can make decisions about where to buy or sell electricity based on the relative costs of delivery. This can lead to more efficient use of the power system and lower costs for consumers. LBMP is an important tool for ensuring the efficient operation of regulated power systems and providing market signals for investment decisions.

The comparative study of LBMP considering all 14 scenarios in the regulated system is shown in Fig. 14. It is seen that after the solar placement in the system the overall LBMP is improved and the quantity of the LBMP improvement is much more considering the higher amount placement of solar power. The impact of solar placement on system economic risk has been studied for the deregulated environment also, similar to the previous case in regulation. The optimal location of solar power can provide additional power generation and extra protection to the electrical system. The revenue, generation cost, and profit comparison with and without placement of solar power in deregulated systems are shown in Fig. 15, Fig. 16, and Fig. 17.

The figures depict the economic progression of the system with solar power installation. The results show that after the placement of maximum quantities of solar power in the system, the system's economic risk is minimized and economic sustainability is maximized. The same scenario is observed for system generation costs, where maximum quantities of solar power provide a minimum generation cost-based system. These results support the incorporation of solar farms with high capacity in a deregulated power system to mitigate system economic risks and maximize system profit.

The comparative study of LBMP considering all 14 scenarios for the deregulated system is shown in Fig. 18. It is seen that after the solar placement in the system the overall LBMP is improved and the quantity of the LBMP improvement is much more considering the higher amount placement of solar power. The deregulated system provides better economic profit to society without considering any renewable energy which further gives much more stability and more economic advancement with the placement of solar plants in the electrical network.

F. STEP 5: OPTIMAL TCSC PLACEMENT

Profit maximization for a regulated system by placement of TCSC (Thyristor Controlled Series Capacitor) is used to improve the efficiency and economic performance of the

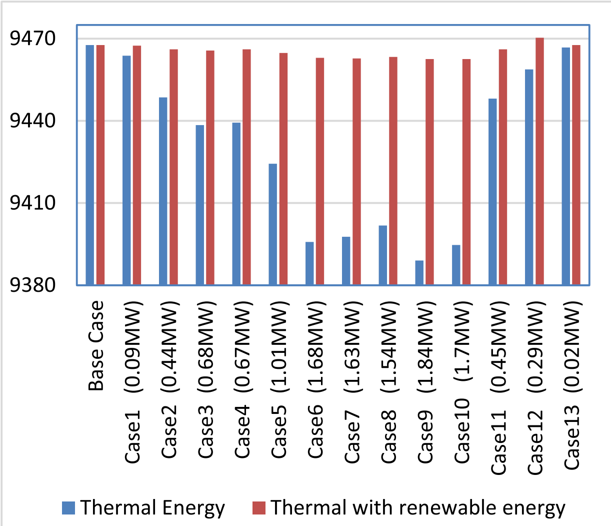

FIGURE 15. Revenue comparison for deregulated system (In $/h).

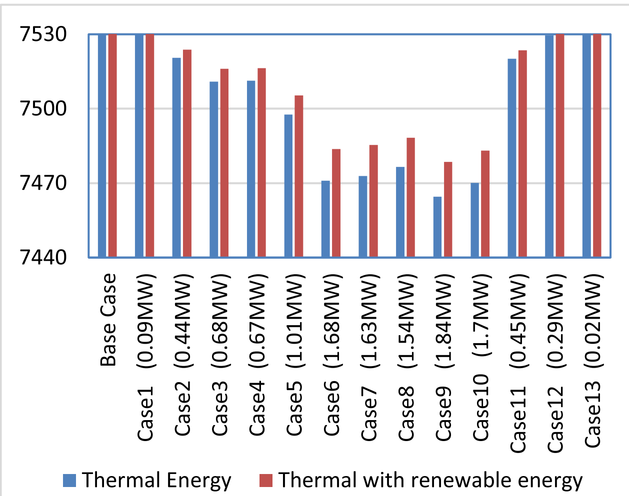

FIGURE 16. Generation cost comparison for deregulated system (In $/h).

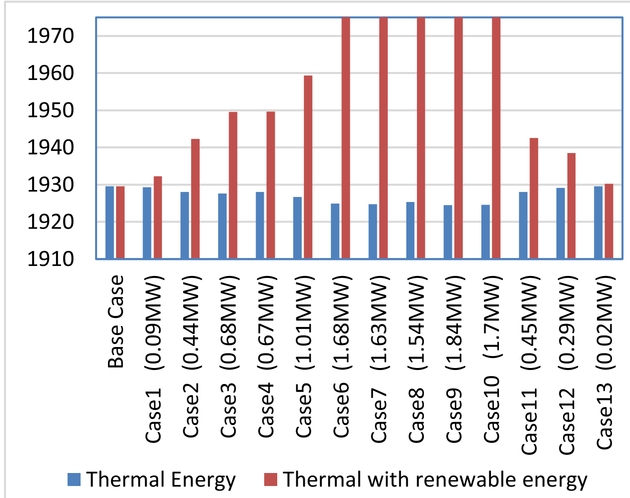

FIGURE 17. Profit comparison for deregulated system (In $/h).

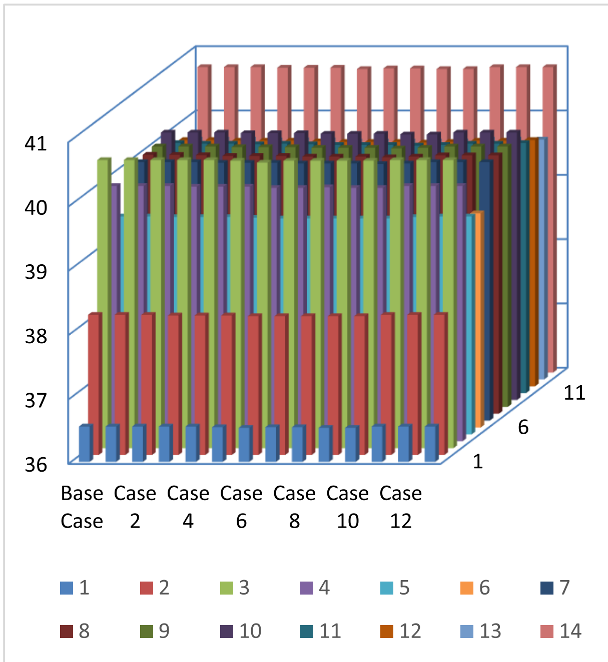

FIGURE 18. LBMP for IEEE14 bus system for deregulated system (In $/MWh).

power system. TCSCs are devices used for power flow control in the power system. They can be used to regulate the voltage and power flow in the transmission network and optimize the use of existing transmission infrastructure. The placement of TCSC involves determining the most cost-effective location and capacity of these devices in the power system. This can be done using various optimization techniques, such as mathematical programming, and genetic algorithms. By the placement of TCSC, the regulated system can reduce transmission losses, increase transmission capacity, and improve voltage stability. This can result in lower operating costs and increased profitability for market participants, such as generators and transmission companies. Furthermore, the placement of TCSC can also help to reduce congestion in the transmission network, which can lead to more efficient use of existing infrastructure and lower costs for consumers. Overall, profit maximization for a regulated system by placement of TCSC is used to improve the economic performance and efficiency of the power system, benefiting both market participants and consumers.

The optimization technique takes into consideration the best placement and minimal value of the objective function for the TCSC. The objective function is measured several times for every possible location for the TCSC to select the optimum location at which the objective function has the lowest value. The placement of the TCSC in the system has been performed based on the techniques stated in Fig. 2. It is found that the TCSC placement will provide the best economic result when the TCSC has been placed at the line connected

TABLE 15. Profit for the regulated system by the placement of TCSC(In $/h).

Case No.	Description	Revenue	Generation Cost	Profit
Base Case	Without solar	1230.032267	899.85	330.182267
TCSC	Solar Without TCSC	1226.947728	894.36	332.5877275
	Solar With TCSC	1241.920845	891.186725	350.7341196

TABLE 16. Profit for the deregulated system by the placement of TCSC (In $/h).

Case No.	Description	Revenue	Generation Cost	Profit
Base Case	Without solar	849.5659422	648.89	200.675942
TCSC	Solar Without TCSC	851.353346	644.68	206.673346
	Solar With TCSC	891.1761964	647.871988	243.3042084

between buses 10 and 11. The profit for the regulated system with and without placement of TCSC has been depicted in Table 15. It has been seen that the system profit is maximized after the placement of TCSC in the system with the operation of solar power.

Profit maximization for a deregulated system by the placement of TCSC is used to improve the economic performance and competitiveness of the power system. In a deregulated system, market participants such as generators and transmission companies operate in a competitive environment. Therefore, profit maximization for these market participants is an important objective. The placement of TCSC can help to achieve this objective by reducing transmission losses, improving transmission capacity, and increasing the efficiency of the power system.

With the placement of TCSC, the deregulated system can improve the economic performance and competitiveness of the power system. The profit for the deregulated system with and without placement of TCSC has been depicted in Table 16. It has been seen that the system profit is exploited after the TCSC installation in the system with the action of solar power.

By the placement of TCSC, the deregulated system can improve voltage stability and reduce the risk of voltage collapse in the transmission network. This can result in improved reliability and quality of power supply to customers, reducing the risk of power outages and other disruptions. Placement of TCSC can also help to reduce transmission losses and increase transmission capacity, which can lead to more efficient use of the transmission network and lower costs for market participants and consumers. Overall, voltage control for a deregulated system by the placement of TCSC is used to improve the reliability, quality, and efficiency of power

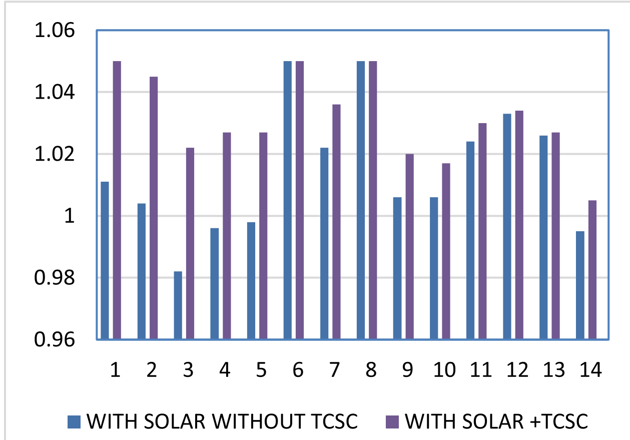

FIGURE 19. Voltage comparison for deregulated system with and without TCSC (In p.u.).

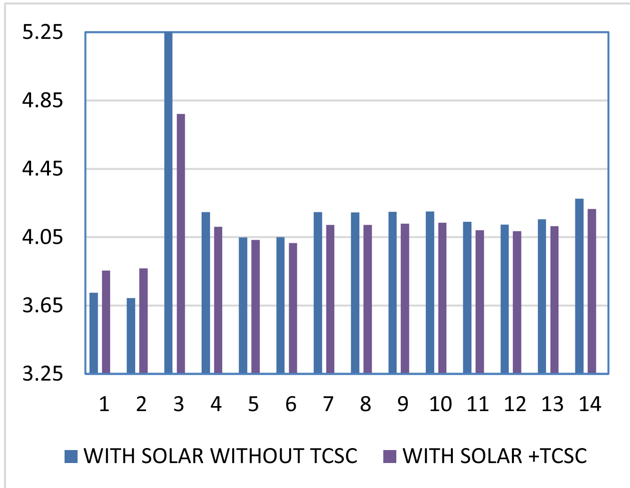

FIGURE 20. LBMP comparison for deregulated system with and without TCSC.

supply, benefiting both market participants and consumers. The comparison of the voltage profiles for the deregulated system with and without the TCSC is shown in Figure 19. After TCSC was added to the system, it was observed that the voltage profile of the deregulated system had improved. Since it is ideal to keep all buses in the system's voltage at 1 pu, Figure 19 shows how the TCSC's positioning drives all buses' voltage levels to go in that direction.

LBMP can be used to reflect the cost savings resulting from the placement of TCSC in the electricity price at different points in the transmission network. This can encourage market participants to invest in the placement of TCSC and other devices that can improve the efficiency of the power system. Furthermore, LBMP can also help to reduce congestion in the transmission network, which can lead to more efficient use of the existing transmission infrastructure and lower costs for market participants and consumers.

Fig. 20 illustrates the LBMPprofile comparison for the deregulated system with and without the installation of TCSC. It is seen that the LBMP profile of the deregulated system is improved after the installation of TCSC in the system. So, the installation of TCSC along with solar power in a deregulated power environment provides economic benefits to the consumer.

G. STEP 6: CALCULATION OF DISEQUILIBRIUM PRICE

In a deregulated power system, solar plants are required to submit their expected power generation scenario to the ISO before the date of operation. Based on this submitted data, ISO schedules power generation from different generating stations. However, due to the uncertain nature of solar irradiance & temperature, solar plants may not be able to generate the scheduled power, leading to a violation of market contracts and an economic burden on the generating companies has been occurred known as disequilibrium prices. The disequilibrium price is calculated for every variation in expected and real solar irradiance and temperature, reflecting the mismatch between expected and real solar data.

The disequilibrium price is maximum when the difference between expected and real solar data is maximum. When the expected solar power is larger than the real solar power, the shortfall charge rate arises, and when the real solar power is larger than the expected solar power, the extra charge rate occurs. The shortfall and extra charge rates are zero when the expected and real solar power are the same. Using the shortfall and extra charge rates, the total disequilibrium price of the electrical system can be calculated. The disequilibrium price is negative when ISO imposes a penalty on the generating station for their shortfall supply of power from renewable sources, and positive when ISO provides a reward to the generating station for their extra supply of power from renewable energy sources.

The expected and real solar power data for 24-hour scenarios are displayed in Table 17. It has been seen that in some hours the expected solar power is more, the real solar power is more in some periods and in some hours both the expected & real solar power are the same. So, there is a chance for the occurrence of positive, negative, and zero disequilibrium prices in the system. The disequilibrium price can directly control the profit of the system.

Table 18 displays the system profit for the deregulated system by considering the disequilibrium price for the chosen locations for all 14 cases. From the results, it is seen that the system profit has been minimized in a few cases due to the adverse impact of the disequilibrium price. It is not desirable for any power producers but this happens due to the variable nature of renewable energy sources. To maximize the overall system profit, the cost of the disequilibrium must be reduced. The appropriate renewable forecasting method or energy storage system can reduce the chances of creating a disequilibrium for a power system.

H. STEP 7: FUEL CELL PLACEMENT

The economic evaluations of a solar-fuel cell hybrid system in a deregulated electrical system are provided in this section of the work. Disequilibrium prices have negative consequences on system profit, which is why the fuel cell integrated system is implemented to address this issue. During off-peak load hours and when there is more solar power available, the fuel cell (FC) system uses an electrolyzer to make hydrogen. During other times, the FC system generates electrical energy using hydrogen. The FC system provides an extra amount of power to close the gap between the real and expected solar power schedules. A fixed energy capacity with a 2 MW FC system has been installed at bus number 9, which was chosen based on the reasoning of the highest load linked to that specific bus in the considered system. Table 19 displays the profit for the deregulated system considering disequilibrium prices and the installation of fuel cells in the system. It is found that the system profit has maximized for all the cases after the placement of the fuel cell in the system. This happens due to the use of fuel cells as energy storage devices by reducing the disparity between the expected and real solar power.

TABLE 17. Expected and real solar power data (In MW).

Hour	1	2	3	4	5	6	7	8
Expected Solar Power	0	0	0	0	0	0	0.065	0.47
Real Solar Power	0	0	0	0	0	0	0.09	0.55
Hour	**9**	**10**	**11**	**12**	**13**	**14**	**15**	**16**
Expected Solar Power	0.75	0.72	1.05	1.49	1.75	1.68	1.52	1.7
Real Solar Power	0.68	0.67	1.01	1.68	1.63	1.54	1.84	1.7
Hour	**17**	**18**	**19**	**20**	**21**	**22**	**23**	**24**
Expected Solar Power	0.45	0.34	0.01	0	0	0	0	0
Real Solar Power	0.45	0.29	0.02	0	0	0	0	0

TABLE 18. Profit for the deregulated system based with and without disequilibrium prices (DP) (In $/h).

Case No.	Profit without DP	Profit with DP	Case No.	Profit without DP	Profit with DP
Base case	1929.578	1929.578	Case 7	1977.474	1973.264
Case 1	1932.252	1933.357	Case 8	1975.135	1969.345
Case 2	1942.326	1943.547	Case 9	1983.968	1989.356
Case 3	1949.617	1942.237	Case 10	1979.501	1979.501
Case 4	1949.699	1943.459	Case 11	1942.613	1942.613
Case 5	1959.381	1951.721	Case 12	1938.495	1936.215
Case 6	1979.226	1984.357	Case 13	1930.219	1934.234

I. STEP 8: COMPARISON OF PROFIT WITH DIFFERENT OPTIMIZATION TECHNIQUES

Different optimization techniques, such as Artificial Bee Colony (ABC) have been employed alongside Sequential

TABLE 19. Profit for the deregulated system with disequilibrium prices (DP) AND fuel cell (FC)(In $/h).

Case No.	Profit with DP & without FC	Profit with DP & with FC	Case No.	Profit with DP & without FC	Profit with DP & with FC
Base case	1929.578	1930.235	Case 7	1973.264	1974.421
Case 1	1933.357	1934.954	Case 8	1969.345	1970.752
Case 2	1943.547	1944.237	Case 9	1989.356	1990.436
Case 3	1942.237	1943.728	Case 10	1979.501	1980.929
Case 4	1943.459	1944.797	Case 11	1942.613	1943.992
Case 5	1951.721	1953.531	Case 12	1936.215	1937.527
Case 6	1984.357	1985.664	Case 13	1934.234	1935.621

TABLE 20. Profit for the deregulated system with DP AND FC with different optimization techniques (In $/h).

Case No.	Profit with DP & FC using SQP	Profit with DP & FC using ABC	Case No.	Profit with DP & FC using SQP	Profit with DP & FC using ABC
Base case	1930.235	1935.645	Case 7	1974.421	1979.354
Case 1	1934.954	1939.387	Case 8	1970.752	1975.384
Case 2	1944.237	1949.384	Case 9	1990.436	1995.654
Case 3	1943.728	1948.347	Case 10	1980.929	1985.357
Case 4	1944.797	1949.896	Case 11	1943.992	1948.267
Case 5	1953.531	1958.347	Case 12	1937.527	1942.365
Case 6	1985.664	1990.364	Case 13	1935.621	1940.259

Quadratic Programming (SQP) to test the capabilities and applicability of the given method. The ABC algorithms were chosen randomly along with SQP to check the effectiveness of the presented approach. Instead of ABC, we can choose any other optimization techniques to get the improved system profit. The system profit using various optimization strategies is shown in Table 20 and Fig. 21. Establishing a solar plant with an FC system resulted in better system profitability than doing so without one, according to the findings. The primary innovation of this work is the application of the ABC optimization technique to a solar-FC hybrid system to mitigate the disequilibrium price and diminish the system's economic risk. ABC algorithms outperform the other optimization algorithms for all the considered scenarios in terms of system profit maximization. The installation of the FC system and the use of ABC processes boost the system to profit in the presence of disequilibrium prices.

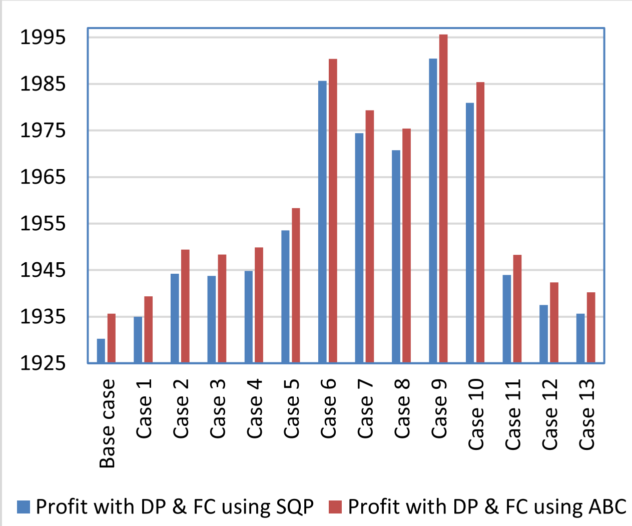

FIGURE 21. Profit comparison for the deregulated system with DP AND FC with different optimization techniques (In $/h).

The SQP has been used for all previous cases (i.e. Stap 1 to Step 7). Here in this section, the ABC optimization method has been implemented along with SQP. From the results, it can be concluded that the placement of TCSC and fuel cells with the operation of ABC can provide better security and safety to the electrical system in terms of economy. It is also concluded that the deregulated system can minimize the profit for the power producer by providing additional economic benefits to society.

VI. CONCLUSION

This work aimed to optimize the profitability of a solar-integrated deregulated power system by incorporating fuel cells and by identifying the optimal placement of TCSC. Through simulations and analysis, it is demonstrated that proper placement of these devices can lead to significant improvements in power flow, voltage stability, and ultimately resulting in increased profits for power generators. The findings of this work highlight the importance of considering not only renewable energy sources but also the critical role of energy storage devices (Fuel cells) and power electronic devices like TCSC in optimizing the performance of the power grid. The results of this study can provide valuable insights for power industry professionals in making informed decisions to maximize their profits while ensuring the stability and efficiency of the power grid. Profits, generation costs, and revenue are calculated and compared for both regulated and deregulated systems. It is observed that the profits are better for the renewable integrated deregulated system. The profit maximization with real-time data for both regulated and deregulated systems has been also calculated. It is observed that when the solar power capacity is more then the profit will be more. The paper concludes that the proposed method is successful in generating the highest profits in the locations under consideration. The optimal placement of TCSC in the proposed system can improve the system efficiency, generation costs, and voltage profiles in deregulated environments. The study outlines a strategy for the optimal operation of a TCSC and fuel cell in a solar-integrated system to maximize system profit and minimize the system's economic risk. The paper also explains how the fuel cell system is employed to offset the solar power integration's deviation in the real-time power market. The ABC algorithm was found to be the best optimization technique in terms of system economic improvement.

ACKNOWLEDGMENT

This work was supported by the Researchers Supporting Project through King Saud University, Riyadh, Saudi Arabia, under Grant RSPD2023R646.

REFERENCES

[1] C. Weber, "Achievements and challenges in European energy markets," *J. Mod. Power Syst. Clean Energy*, vol. 11, no. 3, pp. 1–7, 2023.

[2] M. Dadashi, K. Zare, H. Seyedi, and M. S. Khah, "Coordination of wind power producers with an energy storage system for the optimal participation in wholesale electricity markets," *Int. J. Electr. Power Energy Syst.*, vol. 136, Mar. 2022, Art. no. 107672.

[3] V. A. Evangelopoulos, I. I. Avramidis, and P. S. Georgilakis, "Flexibility services management under uncertainties for power distribution systems: Stochastic scheduling and predictive real-time dispatch," *IEEE Access*, vol. 8, pp. 38855–38871, 2020.

[4] Y. Gao and Q. Ai, "Demand-side response strategy of multi-microgrids based on an improved co-evolution algorithm," *CSEE J. Power Energy Syst.*, vol. 7, no. 5, pp. 903–910, Sep. 2021.

[5] T. Capper, J. Kuriakose, and M. Sharmina, "Impact of energy imbalance on financial rewards in peer-to-peer electricity markets," *IEEE Access*, vol. 10, pp. 55235–55254, 2022.

[6] G. S. Patil, A. Mulla, and T. S. Ustun, "Impact of wind farm integration on LMP in deregulated energy markets," *Sustainability*, vol. 14, no. 7, p. 4354, Apr. 2022.

[7] F. H. Gandoman, A. Ahmadi, A. M. Sharaf, P. Siano, J. Pou, B. Hredzak, and V. G. Agelidis, "Review of FACTS technologies and applications for power quality in smart grids with renewable energy systems," *Renew. Sustain. Energy Rev.*, vol. 82, pp. 502–514, Feb. 2018.

[8] P. Sharma, A. Mishra, A. Saxena, and R. Shankar, "A novel hybridized fuzzy PI-LADRC based improved frequency regulation for restructured power system integrating renewable energy and electric vehicles," *IEEE Access*, vol. 9, pp. 7597–7617, 2021.

[9] K. V. Bhaskar, S. Ramesh, E. Verdú, K. Karunanithi, and S. P. Raja, "An optimal power flow solution to deregulated electricity power market using meta-heuristic algorithms considering load congestion environment," *Electr. Power Syst. Res.*, vol. 214, Jan. 2023, Art. no. 108867.

[10] D. M. Teferra, L. M. H. Ngoo, and G. N. Nyakoe, "Fuzzy-based prediction of solar PV and wind power generation for microgrid modeling using particle swarm optimization," *Heliyon*, vol. 9, no. 1, Jan. 2023, Art. no. e12802.

[11] D. T. Long, T. T. Nguyen, N. A. Nguyen, and L. A. T. Nguyen, "An effective method for maximizing social welfare in electricity market via optimal TCSC installation," *Eng., Technol. Appl. Sci. Res.*, vol. 9, no. 6, pp. 4946–4955, Dec. 2019.

[12] M. Ebeed, A. Mostafa, M. M. Aly, F. Jurado, and S. Kamel, "Stochastic optimal power flow analysis of power systems with wind/PV/TCSC using a developed Runge Kutta optimizer," *Int. J. Electr. Power Energy Syst.*, vol. 152, Oct. 2023, Art. no. 109250.

[13] Prashant, M. Sarwar, A. S. Siddiqui, S. S. M. Ghoneim, K. Mahmoud, and M. M. F. Darwish, "Effective transmission congestion management via optimal DG capacity using hybrid swarm optimization for contemporary power system operations," *IEEE Access*, vol. 10, pp. 71091–71106, 2022.

[14] H. O. Riddervold, E. K. Aasgård, L. Haukaas, and M. Korpås, "Internal hydro- and wind portfolio optimisation in real-time market operations," *Renew. Energy*, vol. 173, pp. 675–687, Aug. 2021.

[15] Z. Zhu, Z. Hu, K. W. Chan, S. Bu, B. Zhou, and S. Xia, "Reinforcement learning in deregulated energy market: A comprehensive review," *Appl. Energy*, vol. 329, Jan. 2023, Art. no. 120212.

[16] M. Farahani, A. Samimi, and H. Shateri, "Robust bidding strategy of battery energy storage system (BESS) in joint active and reactive power of day-ahead and real-time markets," *J. Energy Storage*, vol. 59, Mar. 2023, Art. no. 106520.

[17] M. H. Sulaiman and Z. Mustaffa, "Optimal placement and sizing of FACTS devices for optimal power flow using metaheuristic optimizers," *Results Control Optim.*, vol. 8, pp. 100–145, Sep. 2022.

[18] G. Zhang, S. Zhou, Z. Xie, L. Fan, and J. Gao, "Bi-level power management strategies optimization for multi-stack fuel cell system-battery hybrid power systems," *J. Energy Storage*, vol. 71, Nov. 2023, Art. no. 108066.

[19] F. Peng, X. Xie, K. Wu, Y. Zhao, and L. Ren, "Online hierarchical energy management strategy for fuel cell based heavy-duty hybrid power systems aiming at collaborative performance enhancement," *Energy Convers. Manage.*, vol. 276, Jan. 2023, Art. no. 116501.

[20] P. Shinde, M. R. Hesamzadeh, P. Date, and D. W. Bunn, "Optimal dispatch in a balancing market with intermittent renewable generation," *IEEE Trans. Power Syst.*, vol. 36, no. 2, pp. 865–878, Mar. 2021.

[21] J.-F. Toubeau, J. Bottieau, Y. Wang, and F. Vallée, "Interpretable probabilistic forecasting of imbalances in renewable-dominated electricity systems," *IEEE Trans. Sustain. Energy*, vol. 13, no. 2, pp. 1267–1277, Apr. 2022.

[22] D. Akinyele, E. Olabode, and A. Amole, "Review of fuel cell technologies and applications for sustainable microgrid systems," *Inventions*, vol. 5, no. 3, p. 42, Aug. 2020.

[23] H. Fathabadi, "Novel standalone hybrid solar/wind/fuel cell power generation system for remote areas," *Sol. Energy*, vol. 146, pp. 30–43, Apr. 2017.

[24] M. Shamsi and P. Cuffe, "A prediction market trading strategy to Hedge financial risks of wind power producers in electricity markets," *IEEE Trans. Power Syst.*, vol. 36, no. 5, pp. 4513–4523, Sep. 2021.

[25] Z. Shao, A. H. Ahangarnejad, A. Monazzah, Y. Rao, and D. Rodriguez, "Increasing of fuel cell economic benefits by optimal participation strategy with energy storages and other distributed resources and considering uncertainties and various markets," *Int. J. Hydrogen Energy*, vol. 44, no. 3, pp. 1839–1850, 2019.

[26] V. Mariani, F. Zenith, and L. Glielmo, "Operating hydrogen-based energy storage systems in wind farms for smooth power injection: A penalty fees aware model predictive control," *Energies*, vol. 15, no. 17, p. 6307, Aug. 2022.

[27] O. Utomo, M. Abeysekera, and C. E. Ugalde-Loo, "Optimal operation of a hydrogen storage and fuel cell coupled integrated energy system," *Sustainability*, vol. 13, no. 6, p. 3525, Mar. 2021.

[28] A. Das, S. Dawn, S. Gope, and T. S. Ustun, "A risk curtailment strategy for solar PV-battery integrated competitive power system," *Electronics*, vol. 11, no. 8, p. 1251, Apr. 2022.

[29] S. Dawn, P. K. Tiwari, A. K. Goswami, and R. Panda, "An approach for system risk assessment and mitigation by optimal operation of wind farm and FACTS devices in a centralized competitive power market," *IEEE Trans. Sustain. Energy*, vol. 10, no. 3, pp. 1054–1065, Jul. 2019.

SUBHOJIT DAWN received the M.Tech. degree in power and energy systems engineering and the Ph.D. degree in electrical engineering from the National Institute of Technology Silchar, India. He is currently a Senior Assistant Professor at the Electrical and Electronics Engineering Department, V. R. Siddhartha Engineering College, India. His current research interests include power system economics, renewable energy integration, power system planning, congestion management, smart grid, electricity market, and energy management. He is an Associate Editor of the *Journal of Electrical Engineering and Technology* (JEET) (Springer). He is a continuous Reviewer of many reputed international (SCI/SCIE/ESCI) journals, including *IET Renewable Power Generation*, *IET Generation, Transmission & Distribution*, *Renewable Energy* (Elsevier), and *Applied Energy* (Elsevier). He is an editorial member of several international journals. He is an Editor of *Intelligent Techniques and Applications in Science and Technology* and *Smart and Intelligent Systems* (Springer).

SHREYA SHREE DAS (Graduate Student Member, IEEE) received the M.Tech. degree in power and energy systems engineering from Mizoram University, India, in 2022. She is currently pursuing the Ph.D. degree in renewable energy and power engineering with the School of Electronics Engineering, VIT-AP University, India. Her current research interests include power system economics, renewable energy integration, congestion management, smart grid, electricity market, energy management, and machine learning. She has already published many research papers in international journals (IET, Elsevier, Springer, and T&F) and conferences in the field of power systems and congestion management. She received a Gold Medal for the M.Tech. degree from Mizoram University.

M. RAMESH (Member, IEEE) received the B.Tech. degree in EEE from the Viswanadtha Institute of Technology and Management affiliated with Jawaharlal Nehru Technological University, Hyderabad, in 2002, the M.Tech. degree in advanced power systems from Jawaharlal Nehru Technological University, Kakinada, Andhra Pradesh, in 2005, and the Ph.D. degree in application of artificial intelligent techniques for enhancement of stability in HVDC transmission system from Jawaharlal Nehru Technological University College of Engineering, Ananthapuram, in 2017. He has one year of industrial experience and 19 years of teaching experience and presently working as a Professor at the EEE Department, Marri Laxman Reddy Institute of Technology and Management, Hyderabad. He has published 50 international journals to my credit. He has published ten international and national papers at various conferences held in India and abroad. His research interests include AI techniques, power systems, and FACTS. He is a Life Member of the Indian Society of Technical Education (MISTE), the International Association of Computer Science and Information Technology, and the International Association of Engineers, and a member of the Engineering Council of India (MECI).

SAI RAM INKOLLU received the bachelor's degree in electrical and electronics engineering from Jawaharlal Nehru Technological University, Hyderabad, Andhra Pradesh, India, in 1995, and the master's degree in advanced power systems and the Ph.D. degree in allocation of FACT devices in power systems using novel algorithms from Jawaharlal Nehru Technological University, Kakinada, Andhra Pradesh, in 2005 and 2017, respectively. He is currently working as a Professor in the Department of Electrical and Electronics Engineering, RK College of Engineering, Vijawayada, AP, India. His research interests include power systems operation and control, FACT devices, renewable energy systems, and smart grids. He is a member of the Institute of Engineers, India, and a Life Member of the Indian Society of Technical Education (MISTE), India.

THANDAVA KRISHNA SAI PANDRAJU received the B.Tech. degree in electrical and electronics engineering from Jawaharlal Nehru Technological University, Hyderabad, in 2008, and the M.Tech. degree in power electronics and electric drives from the Vignan Engineering College (now known as Vignan University), Jawaharlal Nehru Technological University, Guntur, in 2011. Currently, he is working as an Assistant Professor with the Department of Electrical and Electronics Engineering, Dhanekula Institute of Engineering and Technology, Ganguru, Vijayawada, affiliated with JNTU Kakinada, Andhra Pradesh, India. He is also a Research Scholar with the Department of Electrical and Electronics Engineering, Faculty of Engineering, Christ (Deemed to be University), Bangalore, Karnataka, India. His research interests include electric power distribution systems with Volt/VAr controls and power system optimization with heuristic algorithms, neural networks, and fuzzy logic applications to power electronics and electrical drives.

FAISAL ALSAIF received the B.Sc. degree in electrical engineering from King Saud University, Riyadh, Saudi Arabia, in 2014, and the M.A.Sc. degree in electrical engineering and the Ph.D. degree in electrical engineering from The Ohio State University, Columbus, OH, USA, in 2017 and 2022, respectively. He is currently working as an Assistant Professor with the Department of Electrical Engineering, College of Engineering, King Saud University, Riyadh, Saudi Arabia. His research interests include power and energy, power electronics, high voltage, smart grids, and power quality improvement.

SAGER ALSULAMY received the Master of Science degree in electrical engineering from the University of Southern California, in 2016, where he gained interest in renewable energy and climate change. He is currently pursuing the Ph.D. degree in energy decarbonization pathways for newly built cities in Saudi Arabia. During the master's degree, he participated in the smart grid regional demonstration project and electrical vehicle program. His previous experience includes working in the utility as an electrical engineer in the distribution sector, testing, and commissioning high to medium-voltage substations, and routine and type tests for different electrical network equipment such as cables, transformers, circuit breakers, and overhead lines. Currently, his research is focused on developing a low-carbon transition pathways plan for a non-grid-connected case study city in Saudi Arabia.

TAHA SELIM USTUN (Member, IEEE) received the Ph.D. degree in electrical engineering from Victoria University, Melbourne, VIC, Australia. He is currently a Researcher with the Fukushima Renewable Energy Institute (FREA), National Institute of Advanced Industrial Science and Technology (AIST), where he leads the Smart Grid Cybersecurity Laboratory. Before that, he was a Faculty Member with the School of Electrical and Computer Engineering, Carnegie Mellon University, Pittsburgh, PA, USA. He has been invited to run specialist courses in South Africa, India, and China. He has delivered talks for the Qatar Foundation, the World Energy Council, the Waterloo Global Science Initiative, and the European Union Energy Initiative (EUEI). His research has attracted funding from prestigious programs in Japan, Australia, the EU, and North America. His current research interests include power systems protection, communication in power networks, distributed generation, microgrids, electric vehicle integration, and cybersecurity in smart grids. He is a member of the IEC Renewable Energy Management WG8 and IEC TC 57 WG17. He serves on the Editorial Board of IEEE Access, IEEE Transactions on Industrial Informatics, *Energies*, *Electronics*, *Electricity*, *World Electric Vehicle Journal*, and *Information* journal.